

RESEARCH ARTICLE

The V2 domain of HIV gp120 mimics an interaction between CD4 and integrin $\alpha_4\beta_7$

Donald Van Ryk¹, Sinmanus Vimompatranon^{1,2}, Joe Hiatt¹, Sundar Ganesan³, Nathalie Chen¹, Jordan McMurry¹, Saadiq Garba¹, Susie Min¹, Livia R. Goes^{1,4}, Alexandre Girard¹, Jason Yolitz¹, Isabella Licavoli¹, Danlan Wei¹, Dawei Huang⁵, Marcelo A. Soares^{4,6}, Elena Martinelli⁷, Claudia Cicala¹, James Arthos^{1*}

1 Laboratory of Immunoregulation, National Institute of Allergy and Infectious Diseases, Bethesda, Maryland, United States of America, **2** Department of Retrovirology, Armed Forces Research Institute of Medical Sciences–United States Component, Bangkok, Thailand, **3** Biological Imaging Section, National Institute of Allergy and Infectious Diseases, Bethesda, Maryland, United States of America, **4** Oncovirology Program, Instituto Nacional de Câncer, Rio de Janeiro, Rio de Janeiro, Brazil, **5** Lymphoid Malignancies Branch, National Cancer Institute, Bethesda, Maryland, United States of America, **6** Department of Genetics, Universidade Federal do Rio de Janeiro, Rio de Janeiro, Brazil, **7** Department of Cell and Developmental Biology, Feinberg School of Medicine, Northwestern University, Chicago, Illinois, United States of America

☞ These authors contributed equally to this work.

* jarthos@niaid.nih.gov



OPEN ACCESS

Citation: Van Ryk D, Vimompatranon S, Hiatt J, Ganesan S, Chen N, McMurry J, et al. (2023) The V2 domain of HIV gp120 mimics an interaction between CD4 and integrin $\alpha_4\beta_7$. *PLoS Pathog* 19(12): e1011860. <https://doi.org/10.1371/journal.ppat.1011860>

Editor: Edward M. Campbell, Loyola University Chicago, UNITED STATES

Received: June 20, 2023

Accepted: November 25, 2023

Published: December 8, 2023

Copyright: This is an open access article, free of all copyright, and may be freely reproduced, distributed, transmitted, modified, built upon, or otherwise used by anyone for any lawful purpose. The work is made available under the [Creative Commons CC0](https://creativecommons.org/licenses/by/4.0/) public domain dedication.

Data Availability Statement: The authors confirm that all data underlying the findings are fully available without restriction. All relevant data are within the paper and its [Supporting Information](#) files.

Funding: This research was supported by the intramural program of the NIAID/NIH. LRG was supported by a grant from Carlos Chagas Filho Rio de Janeiro State Science Foundation (FAPERJ – E-40/200.584/2022). The funders had no role in

Abstract

The CD4 receptor, by stabilizing TCR-MHC II interactions, plays a central role in adaptive immunity. It also serves as the HIV docking receptor. The HIV gp120 envelope protein binds directly to CD4. This interaction is a prerequisite for viral entry. gp120 also binds to $\alpha_4\beta_7$, an integrin that is expressed on a subset of memory CD4⁺ T cells. HIV tropisms for CD4⁺ T cells and gut tissues are central features of HIV pathogenesis. We report that CD4 binds directly to $\alpha_4\beta_7$ in a dynamic way, consistent with a cis regulatory interaction. The molecular details of this interaction are related to the way in which gp120 interacts with both receptors. Like MAdCAM-1 and VCAM-1, two recognized ligands of $\alpha_4\beta_7$, the binding interface on CD4 includes 2 sites (1° and accessory), distributed across its two N-terminal IgSF domains (D1 and D2). The 1° site includes a sequence in the G β -strand of CD4 D2, KIDIV, that binds directly to $\alpha_4\beta_7$. This pentapeptide sequence occurs infrequently in eukaryotic proteins. However, a closely related and conserved sequence, KLDIV, appears in the V2 domain of gp120. KLDIV mediates gp120- $\alpha_4\beta_7$ binding. The accessory $\alpha_4\beta_7$ binding site on CD4 includes Phe⁴³. The Phe⁴³ aromatic ring protrudes outward from one edge of a loop connecting the C'C" strands of CD4 D1. Phe⁴³ is a principal contact for HIV gp120. It interacts with conserved residues in the recessed CD4 binding pocket. Substitution of Phe⁴³ abrogates CD4 binding to both gp120 and $\alpha_4\beta_7$. As such, the interactions of gp120 with both CD4 and $\alpha_4\beta_7$ reflect elements of their interactions with each other. These findings indicate that gp120 specificities for CD4 and $\alpha_4\beta_7$ are interrelated and suggest that selective pressures which produced a CD4 tropic virus that replicates in gut tissues are linked to a dynamic interaction between these two receptors.

study design, data collection and analysis, decision to publish, or preparation of the manuscript.

Competing interests: The authors have declared that no competing interests exist.

Author summary

Integrins modulate cell trafficking and provide costimulatory signals to leukocytes. An increasing number have also been shown to interact in cis with immune receptors. Formation of these multi-receptor complexes is dynamic and typically serves a regulatory function. We report a cis interaction between $\alpha_4\beta_7$, the gut-homing integrin and CD4, a receptor that plays a central role in the adaptive immune response. CD4- $\alpha_4\beta_7$ interactions share features with MAdCAM-1 and VCAM-1, two natural ligands that engage $\alpha_4\beta_7$ in trans. All three receptors engage $\alpha_4\beta_7$ through two discrete sites distributed across their two N-terminal IgSF domains. Specific features of the two $\alpha_4\beta_7$ binding sites on CD4 are related to HIV pathogenesis in a unique and informative way. HIV gp120 binds to both CD4 and $\alpha_4\beta_7$. A key finding of this report is that specific elements of gp120-CD4 and gp120- $\alpha_4\beta_7$ interactions reflect the interaction of these two receptors with each other. We conclude that the selective pressures that resulted in a virus which infects and depletes gut CD4⁺ T cells are linked to CD4- $\alpha_4\beta_7$ cis interactions.

Introduction

The discovery that the HIV gains entry into CD4⁺ T cells by binding directly to the CD4 receptor [1–3], followed by the determination that neutralizing antibodies are directed exclusively to the gp120/41 envelope protein [4], provided a rationale for developing an HIV vaccine immunogen that would elicit CD4 binding site (CD4bs) antibodies. Features intrinsic to envelope-CD4 interactions suppress the elicitation of such antibodies [5,6]. CD4 is comprised of 4 tandemly arrayed Ig-like ectodomains (D1-D4) followed by short transmembrane and cytoplasmic domains [7]. As a first step, gp120 engages a phenylalanine at position 43 (Phe⁴³) in D1 [8,9]. The Phe⁴³ aromatic sidechain protrudes from the edge of an upward facing loop near the apex of CD4 [10]. The CD4bs on gp120 that accommodates Phe⁴³ appears as a spherical cavity. Insertion of Phe⁴³ into this cavity precipitates a significant conformational reorganization of the gp120/41 prefusion trimer [11–14]. This includes the decoupling of the V2 and V3 domains, which in turn facilitates V3-coreceptor engagement and, ultimately, virus fusion with the cell membrane [14–16]. Although we understand gp120-CD4 interactions in detail, the selective pressures that produced this interaction in the first instance remain unclear.

In considering the selective pressures that resulted in a CD4bs on gp120 that engages Phe⁴³ it is useful to consider CD4's normal role. Together with Lck, CD4 transiently migrates into the TCR where it binds to MHC II on APCs and stabilizes TCR interactions [17–19]. Of note, gp120 and MHC II engage CD4 in distinct ways [20]. Substitution of Phe⁴³ eliminates gp120 reactivity but does not disrupt CD4-MHC II interactions [21,22]. Given its exposed presentation, it would appear that Phe⁴³ serves some function. Identifying a natural role for this aa might begin to reveal the selective pressures which resulted in the specialized interaction between gp120 and CD4.

In addition to CD4, the HIV envelope engages several ancillary receptors that may facilitate mucosal transmission. These include DC-SIGN [23], Siglec-1 [24], and the mannose receptor [25]. Because it is difficult to model mucosal transmission in vitro, and even in non-human primates (NHP), the importance of these interactions is subject to debate. Integrin $\alpha_4\beta_7$ ($\alpha_4\beta_7$) is an additional ancillary receptor that we and others have shown binds gp120 [26–29]. $\alpha_4\beta_7$ mediates T cell trafficking to gut associated lymphoid tissues (GALT) via interactions with two adhesion receptors, MAdCAM-1 and VCAM-1, that are expressed on high endothelial venules

that line gut tissues [30,31]. $\alpha_4\beta_7$ is not required for HIV entry or infection, and not all recombinant gp120s bind to it. We have speculated that $\alpha_4\beta_7$ provides a way for HIV to increase transmission efficiency by enhancing access to the plentiful supply of activated CD4⁺ CCR5⁺ T cells in GALT. In support of this proposition, higher frequencies of $\alpha_4\beta_7^{\text{high}}$ CD4⁺ memory T cells correlate with increased susceptibility to HIV acquisition [32]. Additionally, $\alpha_4\beta_7^{\text{high}}$ CD4⁺ memory T cells collected from HIV infected subjects in the early stages of infection (FIEBIG II/III) are enriched in HIV proviral DNA, relative to other CD4⁺ T cell subsets [33], and this same subset is selectively infected and depleted from SIV infected macaques [34]. Finally, an $\alpha_4\beta_7$ -specific mAb was shown to block vaginal transmission of SIV in a repeated low-dose challenge model [35].

In a previous study we determined that $\alpha_4\beta_7$ clusters with CD4 and CCR5 on the surfaces of some $\alpha_4\beta_7^{\text{high}}$ CD4⁺ effector memory T cells [36]. This is puzzling. $\alpha_4\beta_7$ does not play a role MHC II-CD4/TCR interactions. Conversely, there is no direct role for CD4 in $\alpha_4\beta_7$ -mediated T cell trafficking. In this report we show that $\alpha_4\beta_7$ binds directly to CD4 in cis. In this way it adds to the list of integrins that engage counter receptors in both trans (opposing cell) and cis (same cell) [37] (S1A Fig). We find that elements of this interaction are incorporated into the HIV envelope as a means of recognizing both receptors. These findings address the selective pressures that underlie the specific affinity of gp120 for CD4.

Results

HIV gp120 enhances clustering of CD4 and $\alpha_4\beta_7$

CD4, CCR5 and $\alpha_4\beta_7$ colocalize on the surfaces of primary CD4⁺ T cells derived from both colon biopsies and blood derived CD4⁺ T cells cultured in retinoic acid (RA) [36]. To determine whether CD4 and $\alpha_4\beta_7$ come into close-proximity, we carried out a flow-cytometry based proximity ligation assays (PLA) on freshly isolated CD4⁺ T cells using CD4 and β_7 mAbs as probes (S1B Fig). Positive PLA signals indicate a proximity <40nm. Cells were costained with a CD45RA mAb and vedolizumab to distinguish $\alpha_4\beta_7^{\text{high}}$ memory from $\alpha_4\beta_7^{\text{int}}$ naïve cell subsets. We observed positive PLA between CD4 and $\alpha_4\beta_7$ on both subsets, however the frequency of measurable PLA on $\alpha_4\beta_7^{\text{high}}$ memory cells was ~2.5 greater than on naïve CD4⁺ T cells, indicating HIV gp120, like MAdCAM-1, can deliver costimulatory signals through $\alpha_4\beta_7$ in a way that promotes cellular proliferation and HIV infection [38,39]. This finding prompted us to ask whether gp120-mediated signaling might influence CD4- $\alpha_4\beta_7$ clustering. To this end, we employed fluorescence resonance energy transfer (FRET) measured by fluorescence lifetime imaging microscopy (FLIM). Primary CD4⁺ T cells were cultured in the presence of anti CD3, IL-2 and RA for 8 days and then placed on glass coverslips coated with HIV gp120 (stimulated) or without gp120 (unstimulated). Fluorescence lifetime measurements were performed on the CD4 donor mAb tagged with Alexa-488, in the presence or absence of an integrin β_7 acceptor mAb (tagged with Alexa-546). FLIM values were acquired at 20' and 60' time points. Cells treated with gp120 showed a substantial reduction in lifetime signals at 20' and a further reduction at 60' (S1C and S1D Fig). These reductions in the lifetime of the donor indicate proximity of the CD4 and β_7 probes, with an approximate FRETing distances of <15nm, indicating a direct interaction. In considering the role such an interaction might play in CD4⁺ T cell function, we note numerous reports of integrins regulating the activity of other cell surface receptors through direct cis interactions [37] (S1 Fig). A number of these cis interactions involve receptors that, like CD4, present tandem N-terminal Ig-like domains [40–44]. With these reports in mind, we sought to gather additional evidence for a direct physical interaction between CD4 and $\alpha_4\beta_7$.

Specific binding of CD4 to $\alpha_4\beta_7$

The FRET/FLIM results described above indicate a direct interaction between CD4 and $\alpha_4\beta_7$. A determination that CD4 exhibits a specific affinity for $\alpha_4\beta_7$ would support this finding. To this end we employed a fluorescently labelled soluble dodecameric CD4 Ig fusion protein, termed D1D2-Ig α tp, that includes the two N-terminal Ig-like domains of CD4 (D1D2, aa 1–180), followed by IgG1 CH2 and CH3 domains, followed by the 18 aa tail-piece domain of IgA (α tp) [45]. In this oligomer, 12 D1D2-Igs are arranged in a disulphide linked daisy-chain (Fig 1A). Primary CD4⁺ T cells, some of which express $\alpha_4\beta_7$, were reacted with D1D2-Ig α tp

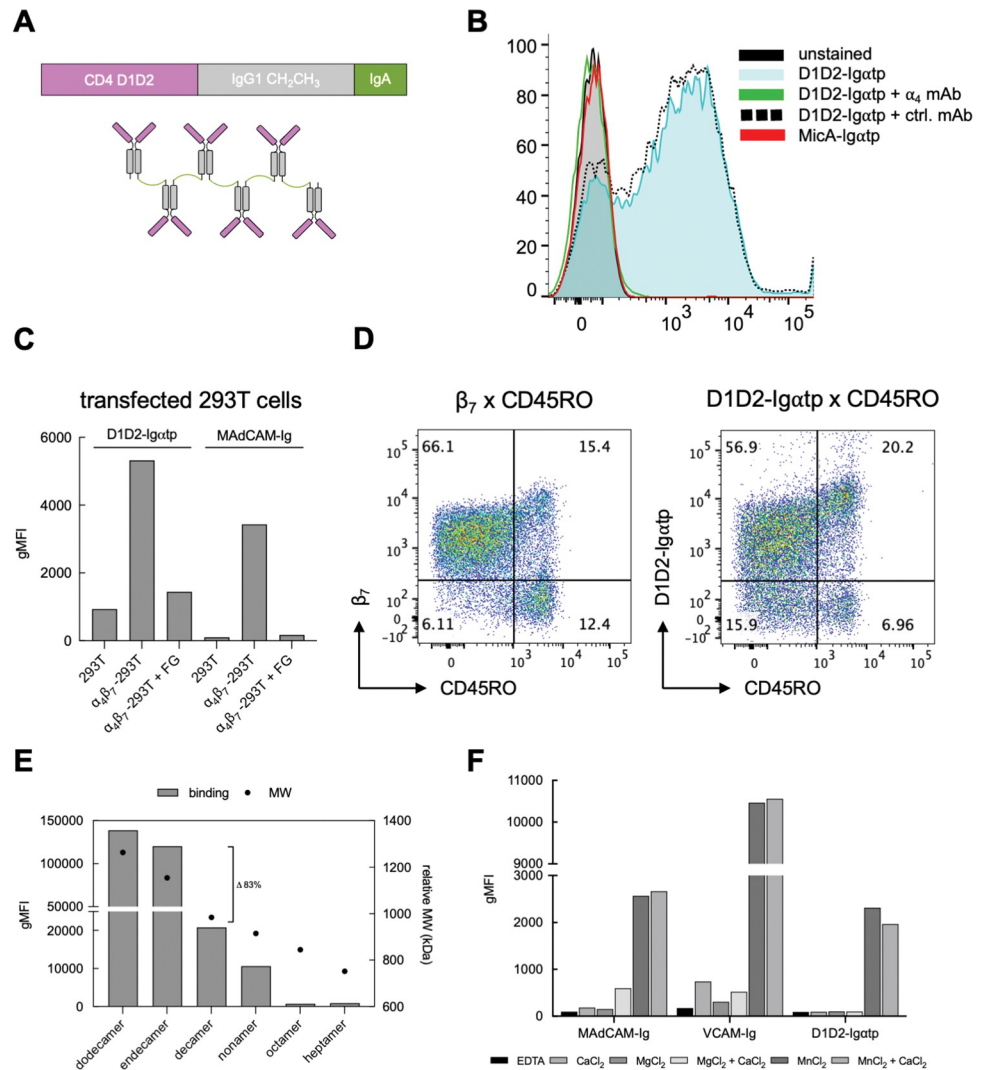


Fig 1. Binding of soluble CD4 to $\alpha_4\beta_7$ on CD4⁺ T cells. (A) Schematic of D1D2-Ig α tp. (B) Flow-cytometry histogram of PE-conjugated D1D2-Ig α tp staining of CD4⁺ T cells alone (blue) or in the presence of either the anti α_4 mAb 2B4 (green) or an irrelevant mAb (black-dashed). Cells stained with PE-conjugated MicA-Ig α tp (red), along with unstained cells (grey) are included. X-axis indicates geometric mean fluorescence intensity (gMFI). (C) 293T cells untransfected or co-transfected with α_4 and β_7 expression vectors stained with either PE-D1D2-Ig α tp or PE-MAdCAM-Ig in the absence or presence of the α_4 antagonist FG. Y-axis indicates gMFI. (D) CD4⁺ T cells stained with anti CD45RO (x-axis) anti β_7 (y-axis) (left), or with anti CD45RO (x-axis) and D1D2-Ig α tp (y-axis) (right). % cells in each quadrant, as indicated. (E) CD4⁺ T cells stained as in B, with lower MW forms of oligomerized D1D2-Ig α tp. Left Y-axis indicates gMFI (bars), right Y-axis indicates relative MW (kDa) (•). (F) Staining of primary CD4⁺ T cells with PE-conjugated D1D2-Ig α tp, PE-MAdCAM-Ig or PE-VCAM-Ig, as in panel B in the presence of buffers containing different combinations of CaCl₂, MgCl₂ and MnCl₂. Y-axis indicates gMFI.

<https://doi.org/10.1371/journal.ppat.1011860.g001>

and analyzed by flow-cytometry. A second oligomeric Ig fusion protein, MicA-Ig α tp, which includes the two N-terminal domains of MicA, was employed as a specificity control. D1D2-Ig α tp, but not MicA-Ig α tp, bound to cells, and this binding was inhibited by an integrin α_4 mAb but not by a control mAb (Fig 1B). To establish specificity, 293T cells were co-transfected with α_4 and β_7 expression vectors and stained with D1D2-Ig α tp in the absence or presence of the 499.5 Da α_4 integrin antagonist firsatgrast (FG) [46]. MAdCAM-Ig was employed as a positive control. Both D1D2-Ig α tp and MAdCAM-Ig bound preferentially to $\alpha_4\beta_7$ transfected cells, and in both cases, binding was inhibited by FG (Fig 1C). We conclude that an oligomeric soluble CD4 that includes only its two N-terminal domains can bind to $\alpha_4\beta_7$ in a specific way.

$\alpha_4\beta_7$ is expressed at intermediate levels on the majority of naïve CD4⁺ T cells in blood. As noted above, most memory CD4⁺ T cells in blood show either little or no $\alpha_4\beta_7$ expression. However a minor subset (~5–20%) express high levels of $\alpha_4\beta_7$. Differential expression of $\alpha_4\beta_7$ on naïve vs memory cell can be visualized by co-staining cells with β_7 and CD45RO mAbs (Fig 1D). We determined that D1D2-Ig α tp bound, like β_7 mAb, to a minor subset of memory cells at relatively high levels, and to naïve cells at a lower level. Although we do not exclude the possibility of trans interactions, the direct interaction we show by FRET/FLIM, combined with the specific binding of CD4 to $\alpha_4\beta_7$ leads us to conclude that CD4 and $\alpha_4\beta_7$ interact in cis on the surface of CD4⁺ T cells (Figs 1 and S1). Molecular details of CD4- $\alpha_4\beta_7$ interactions, described below, support this conclusion.

We next compared the $\alpha_4\beta_7$ reactivity of dodecameric D1D2-Ig α tp to smaller oligomers. While endecamers and decamers bound $\alpha_4\beta_7$ at levels comparable to dodecamers, we observed a marked reduction (~80%) in binding with smaller forms (Fig 1E). We note that for many integrins, including α_4 integrins, ligand recognition is modulated by clustering and avidity effects [47]. Finding that only higher order CD4 oligomers bind $\alpha_4\beta_7$ is consistent with the role that avidity frequently plays in integrin-ligand interactions. Moreover, it helps explain how the specific affinity of CD4 for $\alpha_4\beta_7$ has gone unrecognized until now.

MAdCAM-1 and VCAM-1 bind to the N-terminal headpiece of $\alpha_4\beta_7$ only when it adopts an active conformation [48]. $\alpha_4\beta_7$ conformation is regulated via “inside out signaling” [49], but can be artificially manipulated in vitro by altering relative concentrations of divalent cations. High Mn⁺⁺ concentrations promote an active state. We compared the conformational requirements of CD4 binding to $\alpha_4\beta_7$ with those of MAdCAM-1 and VCAM-1 by staining $\alpha_4\beta_7$ -expressing RPMI8866 cells with D1D2-Ig α tp in 6 buffers supplemented with different combinations of divalent cations. Like MAdCAM-Ig and VCAM-Ig, D1D2-Ig α tp failed to bind $\alpha_4\beta_7$ in the absence of divalent cations (Fig 1F). All three ligands bound to $\alpha_4\beta_7$ in the presence of Mn⁺⁺. We observed low levels of binding of the two natural ligands in the presence of Mg⁺⁺ and no binding of D1D2-Ig α tp. We conclude that D1D2-Ig α tp selectively engages an activated form of $\alpha_4\beta_7$ normally associated with ligand binding.

MAdCAM-1 and VCAM-1 inhibition of CD4 binding to $\alpha_4\beta_7$

Cis interactions between various integrins and leukocyte receptors are known to regulate immune cell functions [37,40–42]. To determine whether CD4 inhibits MAdCAM-1 or VCAM-1 binding to $\alpha_4\beta_7$ we preincubated RPMI8866 cells with labelled MAdCAM-Ig or VCAM-Ig in the presence of increasing concentrations of unlabeled D1D2-Ig α tp. We observed only minor inhibition at high D1D2-Ig α tp concentrations (Fig 2A and 2B). In contrast both MAdCAM-Ig and VCAM-Ig inhibited D1D2-Ig α tp binding to $\alpha_4\beta_7$ in a dose dependent manner (Fig 2C and 2D). This implies that MAdCAM-1 and VCAM-1, acting in trans, may interfere with CD4- $\alpha_4\beta_7$ interactions. What remains unknown is whether

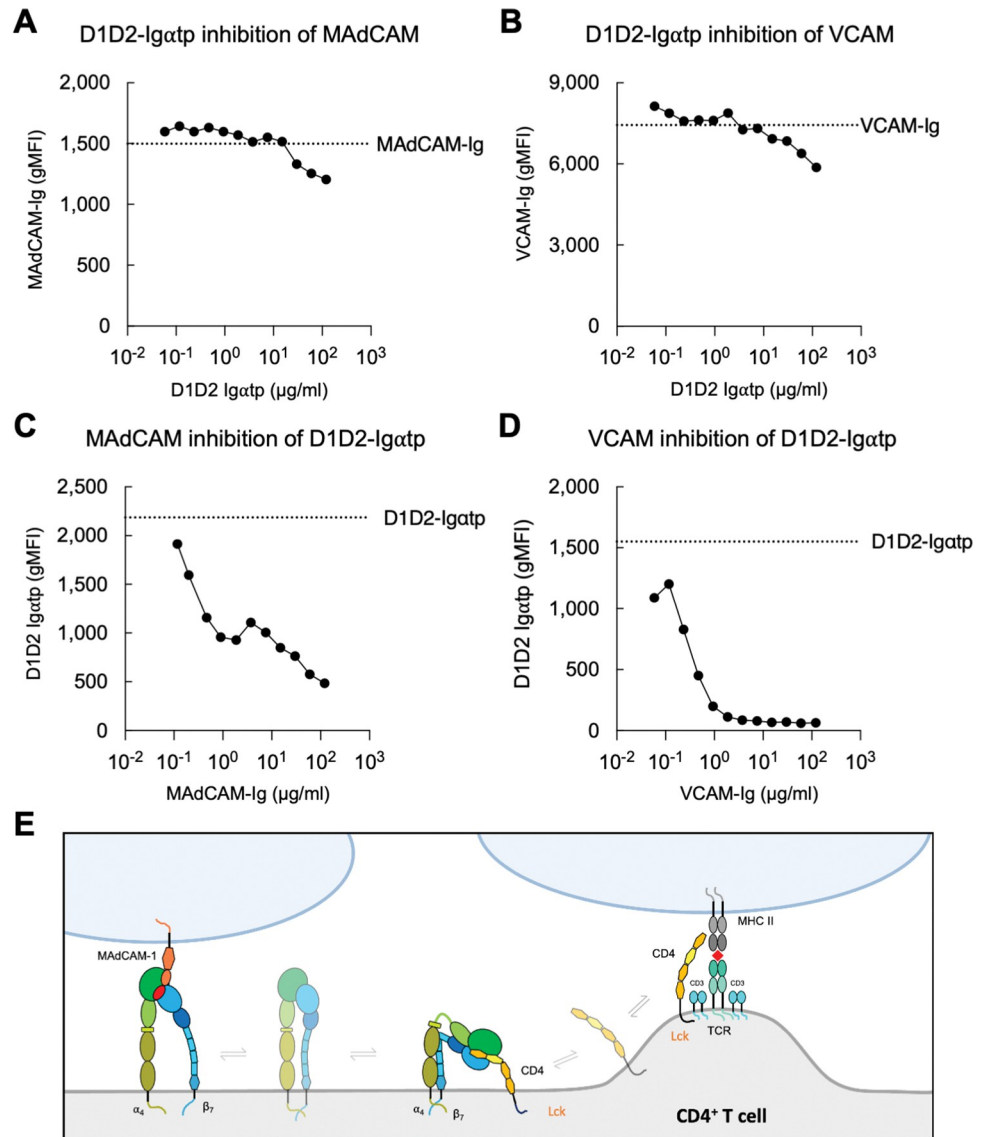


Fig 2. Cross-inhibition of MAdCAM-Ig, VCAM-Ig and D1D2-Ig α tp binding to $\alpha_4\beta_7$. Flow cytometric analysis of (A) PE -conjugated MAdCAM-Ig or (B) PE -conjugated VCAM-Ig binding to RPMI8866 cells pre-incubated with increasing concentrations of unlabeled D1D2-Ig α tp. Cell preincubated with increasing concentrations of (C) unlabeled MAdCAM-Ig or (D) VCAM-Ig followed by PE -conjugated D1D2-Ig α tp. Y-axis indicates gMFI. Dashed line indicates gMFI in the absence of any inhibitor. (E) Schematic of a cis interaction between CD4 D1D2 and the headpiece domain of $\alpha_4\beta_7$ can potentially inhibit $\alpha_4\beta_7$ trans interactions with MAdCAM (left), or CD4 migration into the TCR and trans interactions with MHC II (right).

<https://doi.org/10.1371/journal.ppat.1011860.g002>

interactions between $\alpha_4\beta_7$ and CD4 impact CD4 migration into the TCR and subsequent interactions with MHC II (Fig 2E).

Therapeutics developed to treat inflammatory diseases inhibit CD4 - $\alpha_4\beta_7$ interactions

Several mAbs and small molecule antagonists of $\alpha_4\beta_7$ and $\alpha_4\beta_1$ have been developed to treat diseases, including IBD and MS. Although their specificities vary, they all inhibit $\alpha_4\beta_7$ binding to MAdCAM-1. Vedolizumab and etrolizumab are β_7 mAbs, based on murine mAbs Act-1

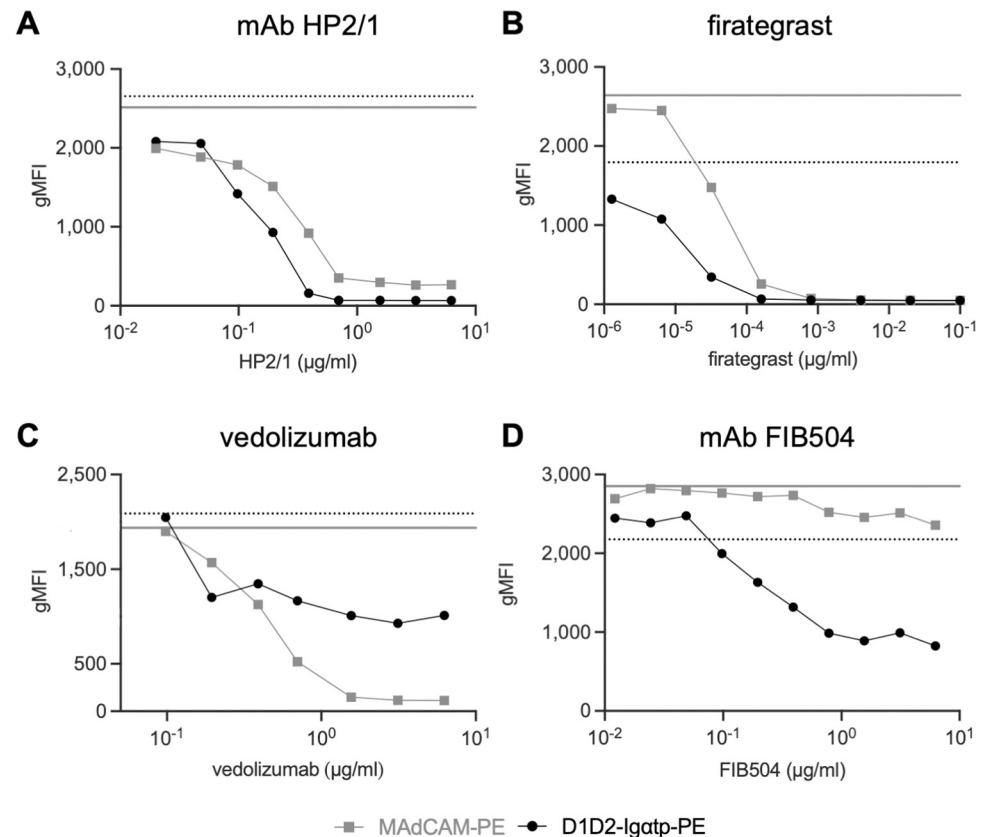


Fig 3. Inhibition of D1D2-Ig α tp and MAdCAM-Ig by α_4 and $\alpha_4\beta_7$ mAb antagonists. Flow-cytometric analysis of $\alpha_4\beta_7^+$ cells stained with PE-conjugated MAdCAM-Ig (grey) or D1D2-Ig α tp (black) in the presence of increasing concentrations of (A) α_4 mAb HP2/1, (B) firtategrast, (C) vedolizumab or (D) β_7 mAb FIB504. Y-axis indicates gMFI. Dashed and solid lines represent gMFI of D1D2-Ig α tp and MAdCAM-Ig respectively, in the absence of any antagonist.

<https://doi.org/10.1371/journal.ppat.1011860.g003>

and FIB504, respectively. Both are used to treat IBDs, [50,51]. Natulizumab is an α_4 specific humanized version of the mouse mAb HP2/1 used to treat Multiple Sclerosis (MS) [52]. FG is a small-molecule MAdCAM-1 and VCAM-1 inhibitor developed to treat MS [46]. To determine whether these antagonists block CD4 binding to $\alpha_4\beta_7$, we stained RPMI8866 cells with D1D2-Ig α tp in the absence or presence of increasing concentrations of each (Fig 3). HP2/1 inhibited both D1D2-Ig α tp and MAdCAM-Ig to near completion at a concentration of 1 μ g/ml. FG also inhibited both ligands. Vedolizumab blocked MAdCAM-Ig efficiently at 1 μ g/ml but was only able to reduce D1D2-Ig α tp binding ~50% at a concentration of 10 μ g/ml. FIB504 partially inhibited (~60% at 10 μ g/ml) D1D2-Ig α tp binding to $\alpha_4\beta_7$. In sum, although their patterns of inhibition varied, each of these α_4 and β_7 antagonists interfered with CD4- $\alpha_4\beta_7$ interactions.

Peptide scanning of the $\alpha_4\beta_7$ binding site(s) on CD4 D1D2

To measure the specific affinity of CD4- $\alpha_4\beta_7$ interactions we developed a surface plasmon resonance (SPR) -based assay in which recombinant $\alpha_4\beta_7$ was passed over a surface coated with a 23 kD D1D2 protein (aa 1–183) [8]. For comparison we prepared surfaces with recombinant MAdCAM-Ig, VCAM-Ig, monomeric gp120, and a SOSIP env trimer (S1 Table). Assays were carried out in the presence of MnCl₂ to present $\alpha_4\beta_7$ in an active conformation. We obtained a dissociation constant (KD (M)) between $\alpha_4\beta_7$ and CD4 of 3.57×10^{-9} . This rate of dissociation was

similar to that of both MAdCAM-Ig and VCAM-Ig with $\alpha_4\beta_7$ and is indicative of a relatively high-affinity interaction.

We next modified our SPR -based assay in order to map the site(s) on CD4 that interacts with $\alpha_4\beta_7$. In this modified assay $\alpha_4\beta_7$ was passed over a surface coated with CD4 D1D2 in the absence or presence of 42 overlapping 15 amino acid linear peptides spanning CD4 residues 1–178 (S2 Table). Two peptides located in CD4 D1, #7 and #9, inhibited $\alpha_4\beta_7$ binding by ~17% (Fig 4A). The final peptide in CD4 D2, p42, inhibited binding by ~ 66%. Linear peptides often lack the true conformation of the protein from which they are derived. Additionally, the kinetic format of our assay allows for ligand-analyte rebinding during the association phase.

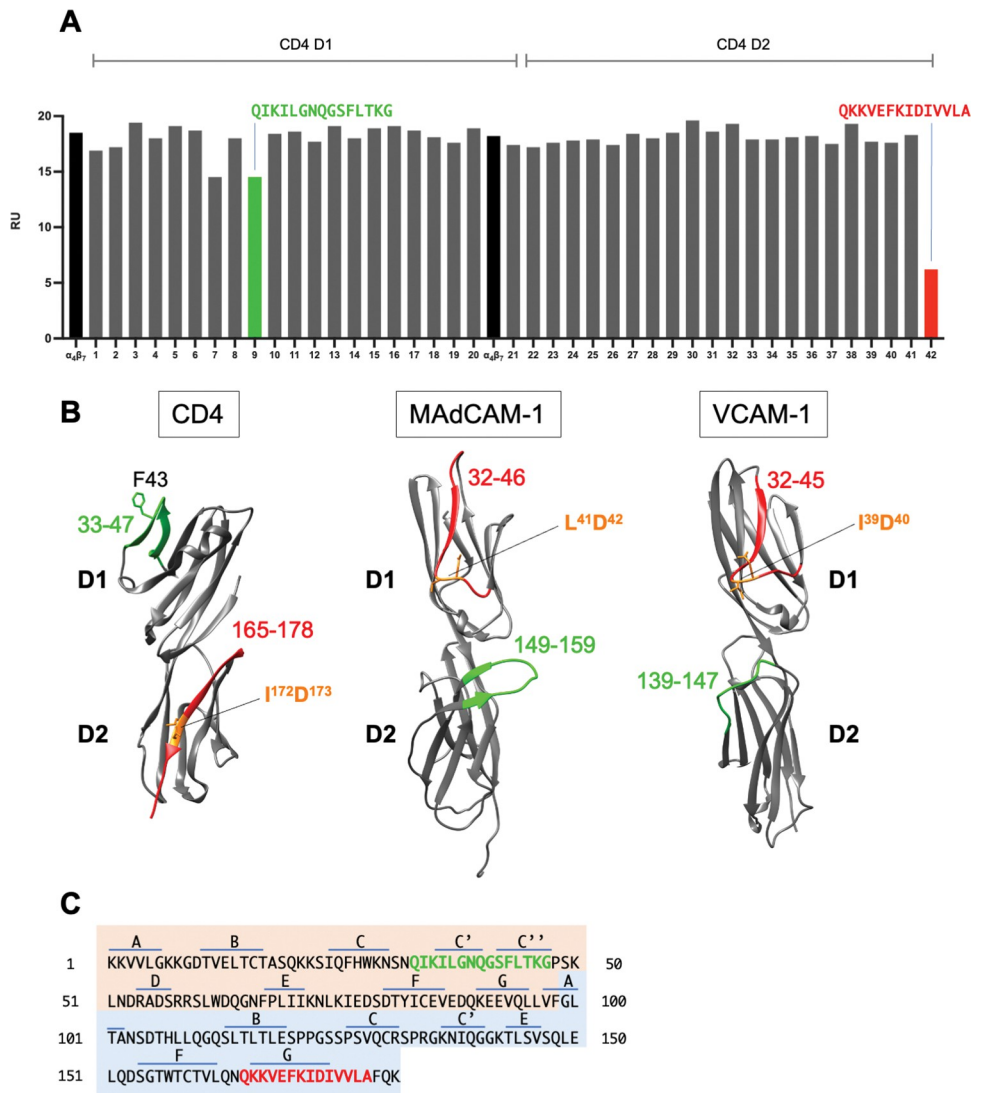


Fig 4. CD4 peptide inhibition of soluble $\alpha_4\beta_7$ binding to CD4 D1D2. (A) SPR assay of soluble $\alpha_4\beta_7$ binding to a biosensor surface coated with sCD4 D1D2 in the absence (black) or presence of overlapping 15 aa peptides corresponding to residues encoded in CD4 D1 (p1-p21) and D2 (p22-p42). Binding of $\alpha_4\beta_7$ to the D1D2 coated surface is reported in response units (RU). p9 (green) and p42 (red) aa sequences are reported. (B) Ribbon diagram of D1 and D2 domains of CD4 (PDB: 1CDI), MAdCAM-1 (PDB: 1BQS) and VCAM-1 (PDB: 1IJ9). 1° binding sites are highlighted in red, and accessory binding sites are highlighted in green. Predicted metal ion coordination sites for each ligand are indicated (orange). (C) CD4 D1D2 residues with β -strand designations listed above. D1 residues are highlighted in orange and D2 residues in blue. p9 and p42 are highlighted in red and green.

<https://doi.org/10.1371/journal.ppat.1011860.g004>

These features render this inhibition assay somewhat insensitive. Nevertheless, the dynamic range of this assay is sufficient to identify interactions that are worthy of follow-up investigation (S4 Fig). As such, our preliminary findings raised the possibility that both D1 and D2 domains of CD4 interact with $\alpha_4\beta_7$. Of note, MAdCAM-1 and VCAM-1, like CD4, present two tandemly arrayed N-terminal IgSF domains (Fig 4B). In both cases, binding to $\alpha_4\beta_7$ is mediated by a 1° binding site in their D1s and an accessory site, located in their D2s. The term accessory is a misnomer insofar as these sites play an essential role in $\alpha_4\beta_7$ binding. Follow-up experiments focused on p9 and p42, which we herein refer to as pCD4³³⁻⁴⁷ and pCD4¹⁶⁵⁻¹⁷⁸. pCD4³³⁻⁴⁷ partially overlaps the D1 C' C'' β -strands and a connecting loop. The primary gp120 contact site (Phe⁴³) lies at the N-terminal edge of this loop (Fig 4C). pCD4¹⁶⁵⁻¹⁷⁸ includes Q¹⁶⁵ and K¹⁶⁶. These residues lie primarily within the G β -strand of D2, close to the boundary with D3. Because peptide inhibition assays sometime mediate nonspecific effects, further analysis was performed to better establish the role of these two regions of CD4 in binding to $\alpha_4\beta_7$.

CD4¹⁶⁵⁻¹⁷⁸ binds directly to $\alpha_4\beta_7$

To further investigate the interaction between pCD4¹⁶⁵⁻¹⁷⁸ and $\alpha_4\beta_7$ we attached a fluorescein dye to its amino terminus via a trioxatridecan-succinamic acid (Ttds) linker (Fig 5A). A scrambled pCD4¹⁶⁵⁻¹⁷⁸ was employed as a control. Both peptides were reacted with RA -treated primary CD8⁺ T cells that express high levels of $\alpha_4\beta_7$. pCD4¹⁶⁵⁻¹⁷⁸ reacted strongly in the presence, but not in the absence of Mn⁺⁺ (Fig 5B). The scrambled pCD4¹⁶⁵⁻¹⁷⁸ showed limited binding (Fig 5C). α_4 mAbs 2B4 and HP2/1 reduced binding by ~80%, as did FG, FIB504 and vedolizumab inhibited binding by ~50%. This inhibition pattern resembles the one we obtained when inhibiting D1D2-Ig α tp with the same antagonists (Fig 3). We conclude that the CD4 D2 G β -strand binds directly to the headpiece region of $\alpha_4\beta_7$ in a cation dependent manner. Support for this conclusion, in the form of site directed mutagenesis within the D2 G β -strand is provided below.

CD4¹⁶⁵⁻¹⁷⁸ shares a sequence motif with gp120 V2

MAdCAM-1, VCAM-1 and fibronectin each encode an essential aliphatic aa-Asp motif in their 1° ligand binding site (MAdCAM-1: LD, VCAM-1: ID, fibronectin: LD). The Asp coordinates with a Mg⁺⁺ ion that sits in an $\alpha_4\beta_7$ metal ion -dependent adhesion site (MIDAS). pCD4¹⁶⁵⁻¹⁷⁸ includes such a motif: I¹⁷²D¹⁷³, consistent with its cation -dependent binding to $\alpha_4\beta_7$. Using I¹⁷² and D¹⁷³ as anchor residues we aligned pCD4¹⁶⁵⁻¹⁷⁸ to the MAdCAM-1 and VCAM-1 1° ligand binding sites [53,54], but found no additional sequence similarity (Fig 6A).

We and others have previously reported that some recombinant gp120s bind to $\alpha_4\beta_7$ in a cation -dependent manner [26–28,55,56] and determined that this interaction is mediated by conserved residues in the V2 domain. In support of this finding, a subtype B V2 consensus peptide spanning residues 170–184 (pV2¹⁷⁰⁻¹⁸⁴) inhibits gp120 binding to $\alpha_4\beta_7$ [56]. pV2¹⁷⁰⁻¹⁸⁴ includes a conserved aliphatic aa-Asp motif (L¹⁷⁹D¹⁸⁰). Substitution of L¹⁷⁹D¹⁸⁰ reduces gp120 binding to $\alpha_4\beta_7$ substantially [26]. Cardozo and colleagues showed, using a similar V2 peptide, that aa 170–172 (consensus QK[VE]) also plays a key role in gp120 binding to $\alpha_4\beta_7$ [28]. With these observations in mind, we aligned pCD4¹⁶⁵⁻¹⁷⁸ with pV2¹⁷⁰⁻¹⁸⁴ (Fig 6B). Sequence similarity was evident. Most striking, CD4 residues 171–175 (KIDIV) are similar to V2 residues 178–182 (KLDVV). In V2, K¹⁷⁸, L¹⁷⁹ and D¹⁸⁰ are the most frequently encoded amino acids at their respective positions (Fig 6C). Although V¹⁸¹ in our subtype B V2 peptide does not align with CD4 I¹⁷⁴, the presence of valine at this position is atypical. The majority of gp120s (61%) in the Los Alamos National Laboratory (LANL) database encode either an isoleucine or leucine at position 181, such that the CD4 D2 sequence KIDIV is nearly identical to KLDIV, the most

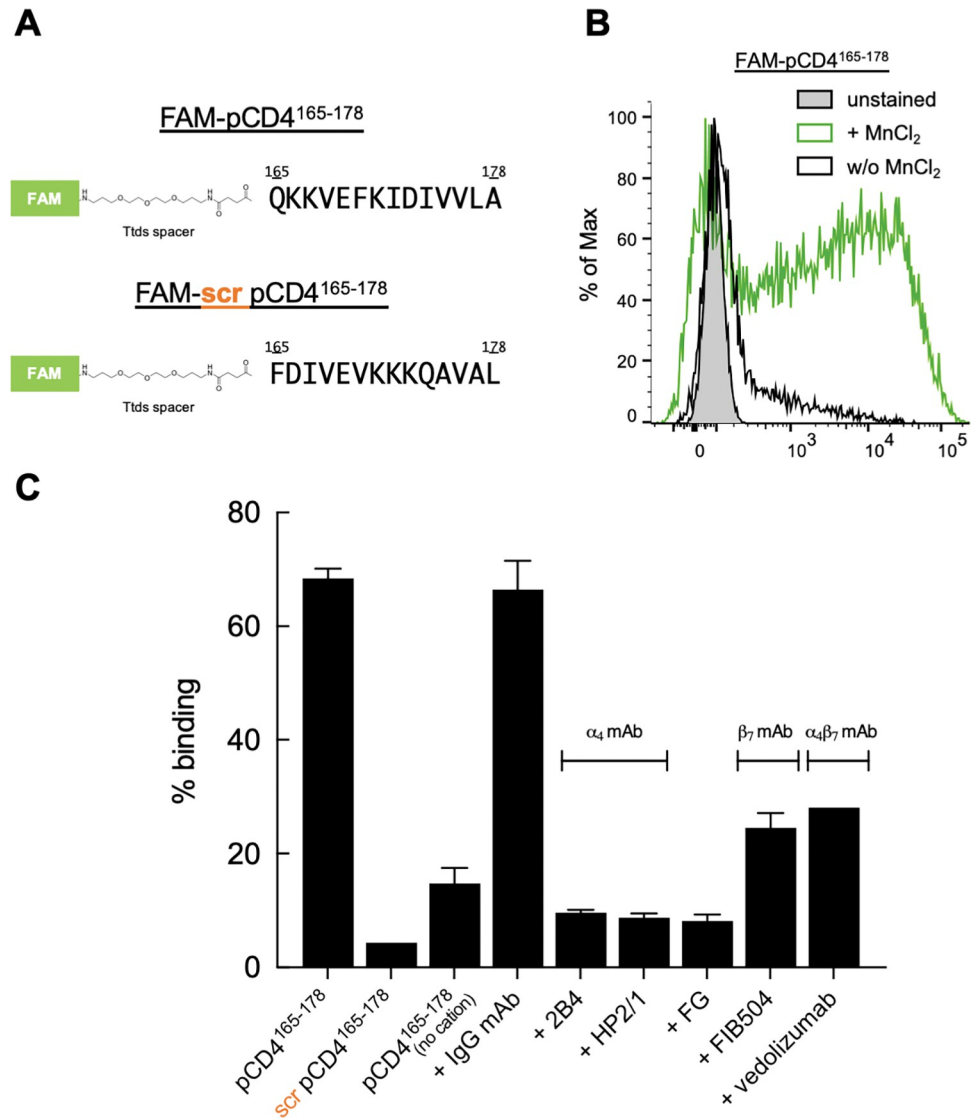


Fig 5. Direct binding of pCD4¹⁶⁵⁻¹⁷⁸ to $\alpha_4\beta_7$ on primary T cells. (A) Sequence of FAM-conjugated pCD4¹⁶⁵⁻¹⁷⁸ and a scrambled derivative (FAM-scr pCD4¹⁶⁵⁻¹⁷⁸). (B) Flow-cytometry derived histogram of pCD4¹⁶⁵⁻¹⁷⁸ binding to RA-cultured CD8⁺ T cells. pCD4¹⁶⁵⁻¹⁷⁸ in the presence (green), or absence of Mn²⁺ (black). Unstained cells are shown (grey). (C) Binding of pCD4¹⁶⁵⁻¹⁷⁸ and its scrambled derivative to CD8⁺ T cells in the presence of MnCl₂ as in panel B, and in the presence of α_4 and $\alpha_4\beta_7$ antagonists, as indicated. Y-axis indicates % cells bound. Error bars represent standard error from 3 independent experiments.

<https://doi.org/10.1371/journal.ppat.1011860.g005>

common V2 sequence spanning aa 178–182, and both include a metal ion coordination motif (ID and LD). Three additional conserved residues in this region of V2, Q¹⁷⁰, K¹⁷¹, and F¹⁷⁶ could also be aligned with residues in pCD4¹⁶⁵⁻¹⁷⁸. In sum, a sequence overlapping the G β -strand of CD4 D2, that binds directly to $\alpha_4\beta_7$, is nearly identical to a conserved sequence in gp120 V2 that also binds to $\alpha_4\beta_7$.

Inspection of nonhuman primate orthologs indicates that CD4 residues Q¹⁶⁵, K¹⁶⁶, F¹⁷⁰, along with KIDIV (aa 171–175) are conserved in 19 of 21 Old World monkeys, including those of Asian origin that are employed in NHP models of HIV infection, but are absent in New World monkeys and other mammals (Figs 6D, 6E and S3).

then restricted our search to include only KIDIV. The probability that this sequence appears randomly is 30 per 100,000 ($p = 3e^{-5}$). We observed 41 hits among 560,000 proteins. 8 were primate CD4 genes. The only other cell surface receptor encoding KIDIV was IL-1R, which does not react with $\alpha_4\beta_7$. This suggests that other elements of CD4 D2 are necessary for $\alpha_4\beta_7$ reactivity. These findings indicate that a CD4 D2 sequence that binds directly to $\alpha_4\beta_7$ is not common in the eukaryotic proteome, indicating that the presence of a closely related sequence in the gp120 V2 domain was worthy of further investigation.

CD4¹⁶⁵⁻¹⁷⁸ and V2¹⁷⁰⁻¹⁸⁴ cross-inhibit $\alpha_4\beta_7$ ligands

The sequence similarity between pCD4¹⁶⁵⁻¹⁷⁸ and pV2¹⁷⁰⁻¹⁸⁴ suggested that they engage the $\alpha_4\beta_7$ headpiece in a similar way. To determine if this is the case, we employed an SPR-based assay. Biosensor surfaces were coated with either CD4 D1D2 or a 42 aa cyclic V2 peptide derived from the subtype E 92TH023 gp120 (cV2 92TH023). A third surface coated with MAdCAM-Ig was employed as a positive control. Soluble $\alpha_4\beta_7$ was passed over these surfaces. We then evaluated the capacity of staggered 15 aa peptides that span either CD4 D2 or gp120 V2 to inhibit this interaction (Fig 7A).

Before proceeding, we evaluated CD4 peptides p43, p44 and p45 that extend our initial screen presented in Fig 4A to include residues in D2 c-terminal to A¹⁷⁸, the final residue in pCD4¹⁶⁵⁻¹⁷⁸. p44 and p45 were unable to inhibit $\alpha_4\beta_7$ binding to D1D2 (Fig 7B), indicating that CD4 residues c-terminal to A¹⁷⁸ do not likely contribute to $\alpha_4\beta_7$ reactivity. p43 showed reduced inhibition relative to pCD4¹⁶⁵⁻¹⁷⁸, suggesting that Q¹⁶⁵ and K¹⁶⁶, which are absent in p43 but present in pCD4¹⁶⁵⁻¹⁷⁸, contribute to the $\alpha_4\beta_7$ reactivity. This is notable because these two residues align with gp120 V2 aa Q¹⁷⁰K¹⁷¹, which were singled out by Cardozo and colleagues as key determinants of V2- $\alpha_4\beta_7$ reactivity [28].

We previously reported that pV2¹⁷⁰⁻¹⁸⁴ inhibits A244 gp120 binding to $\alpha_4\beta_7$ [56], and reproduced that result here for reference (Fig 7C). We then determined that pV2¹⁷⁰⁻¹⁸⁴ inhibits D1D2 binding to $\alpha_4\beta_7$ (Fig 7D), and pCD4¹⁶⁵⁻¹⁷⁸ inhibits gp120 binding to $\alpha_4\beta_7$ (Fig 7E). Finally, both pCD4¹⁶⁵⁻¹⁷⁸ and pV2¹⁷⁰⁻¹⁸⁴ inhibit MAdCAM-Ig binding to $\alpha_4\beta_7$ (Fig 7F and 7G). In summary, pCD4¹⁶⁵⁻¹⁷⁸ and pV2¹⁷⁰⁻¹⁸⁴ interchangeably inhibit gp120, CD4 D1D2, and MAdCAM-Ig binding to $\alpha_4\beta_7$. Considering that CD4 is relatively invariant, and gp120 V2 is under continuous selection, we conclude that gp120 V2 mimics the G β -strand of CD4 D2.

As presented in S3 Fig the G β -strand of CD4 D2 is well conserved in Old World monkeys, but not in New World monkeys. Because divergent sequences can adopt similar structures, we asked whether a D2 G β -strand peptide derived from a New World monkey CD4 could retain a structure required to bind $\alpha_4\beta_7$. *Aotus nancymaae* is a South American night monkey whose D2 G β -strand sequence diverges from human CD4 in a significant way. An *Aotus* peptide analogous to pCD4¹⁶⁵⁻¹⁷⁸ was employed as an inhibitor of $\alpha_4\beta_7$ binding to surface immobilized D1D2, as described above. We included a Gorilla pCD4¹⁶⁵⁻¹⁷⁸, which differs slightly from human CD4, as a reference. The *Aotus* and Gorilla peptides both inhibited $\alpha_4\beta_7$ binding in a similar way (S5 Fig). This suggests that the cis interaction between $\alpha_4\beta_7$ and CD4 is retained in *Aotus*, and perhaps other New World monkeys and demonstrates that $\alpha_4\beta_7$ can retain CD4 binding even with a sequence that diverges significantly from the conserved KIDIV sequence. This observation is consistent with gp120 V2 mimicking CD4 when one considers that HIV evolved out of Old World monkeys.

A gp120 binding residue in CD4 D1 mediates $\alpha_4\beta_7$ -reactivity

Both MAdCAM-1 and VCAM-1 utilize two binding sites (1° and accessory) to engage $\alpha_4\beta_7$. Our preliminary peptide scan (Fig 4) indicated that pCD4³³⁻⁴⁷, which overlaps a loop

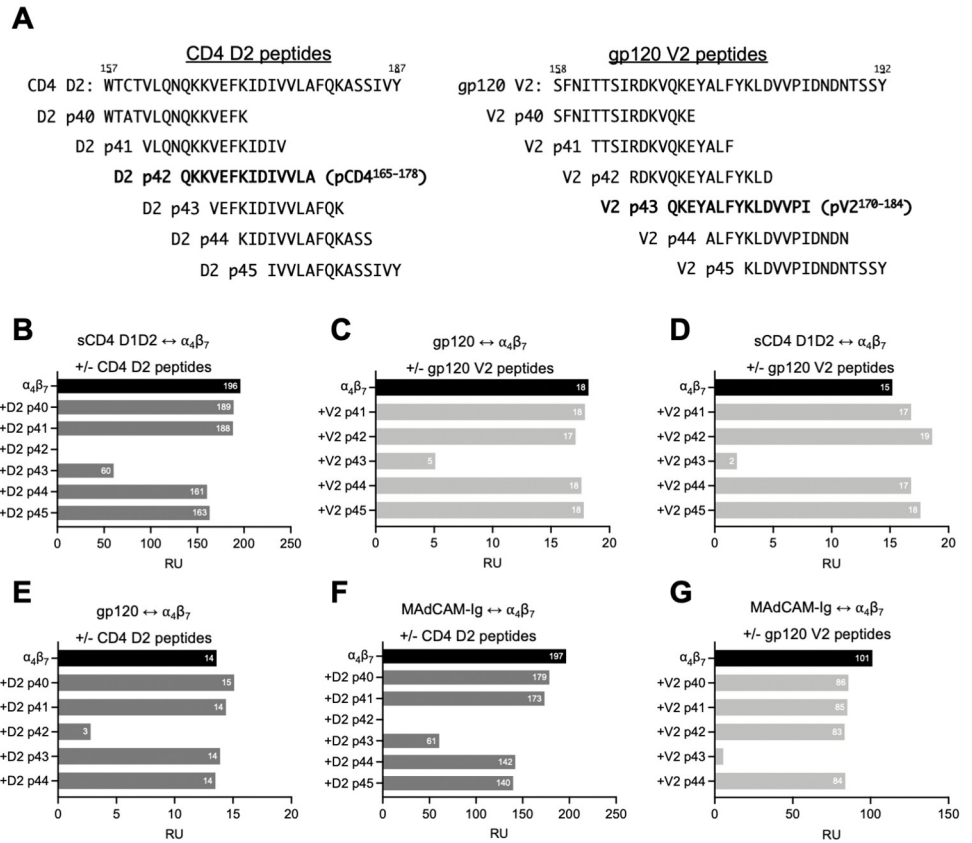


Fig 7. Reciprocal inhibition of gp120 V2 and CD4 binding to $\alpha_4\beta_7$ by D2 and V2 peptides. SPR measurements of soluble $\alpha_4\beta_7$ (analyte) binding to biosensor surfaces coated with CD4 D1D2, 92TH023 cyclic peptide, or MAdCAM-Ig in the absence or presence of either CD4 D2 or gp120 V2 peptides, as indicated. (A) List of overlapping 15 aa peptides corresponding to residues 157–187 of CD4 and residues 158–192 of gp120 V2 (subtype B consensus sequence). (B) Binding of $\alpha_4\beta_7$ to sCD4 D1D2 +/- CD4 D2 peptides. X-axis indicates $\alpha_4\beta_7$ mass bound (RU) at the end of the association phase. (C) Binding of $\alpha_4\beta_7$ to 92TH023 +/- gp120 V2 peptides. (D) Binding of $\alpha_4\beta_7$ to sCD4 D1D2 +/- gp120 V2 peptides. (E) Binding of $\alpha_4\beta_7$ to 92TH023 +/- CD4 D2 peptides. (F) Binding of $\alpha_4\beta_7$ to MAdCAM-Ig +/- CD4 D2 peptides. (G) Binding of $\alpha_4\beta_7$ to MAdCAM-Ig +/- gp120 V2 peptides.

<https://doi.org/10.1371/journal.ppat.1011860.g007>

connecting the C'-C'' strands in D1, inhibited $\alpha_4\beta_7$ binding in a modest way (~17%). This observation, by itself, is insufficient to conclude that CD4 D1 is involved in binding to $\alpha_4\beta_7$. However, with MAdCAM-1 and VCAM-1 in mind, we explored this possibility further. MAdCAM-1 and VCAM-1 accessory sites, which are both loops, were initially identified by site directed mutagenesis [53,54]. Mutating these accessory sites reduced their $\alpha_4\beta_7$ reactivity dramatically. We followed a similar strategy for CD4 by constructing S42G/F43V-D1D2-Ig α tp, which incorporates mouse CD4 substitutions (Fig 8A). Phe⁴³ is of interest because it is the primary contact for gp120. In previous studies an S42G/F43V CD4 D1D2 mutant was shown to fully abrogate CD4-gp120 interactions without disrupting the overall conformation of D1D2 [8,57]. We constructed an additional CD4 D2 mutant, K171D, that incorporates a substitution within the KIDIV sequence in the D2 G β -strand, expecting that it would disrupt $\alpha_4\beta_7$ binding and serve as a control. Wild type and mutant dodecamers were reacted with $\alpha_4\beta_7$ -expressing CD8⁺ T cells. D1D2-Ig α tp bound to $\alpha_4\beta_7$ in a dose dependent manner (Fig 8B). K171D D1D2-Ig α tp showed reduced binding to $\alpha_4\beta_7$. Of note, S42G/F43V-D1D2-Ig α tp showed an even greater reduction in reactivity, suggesting that a region of CD4 D1 that includes the C'C'' strands and a connecting loop mediates the CD4- $\alpha_4\beta_7$ interaction.

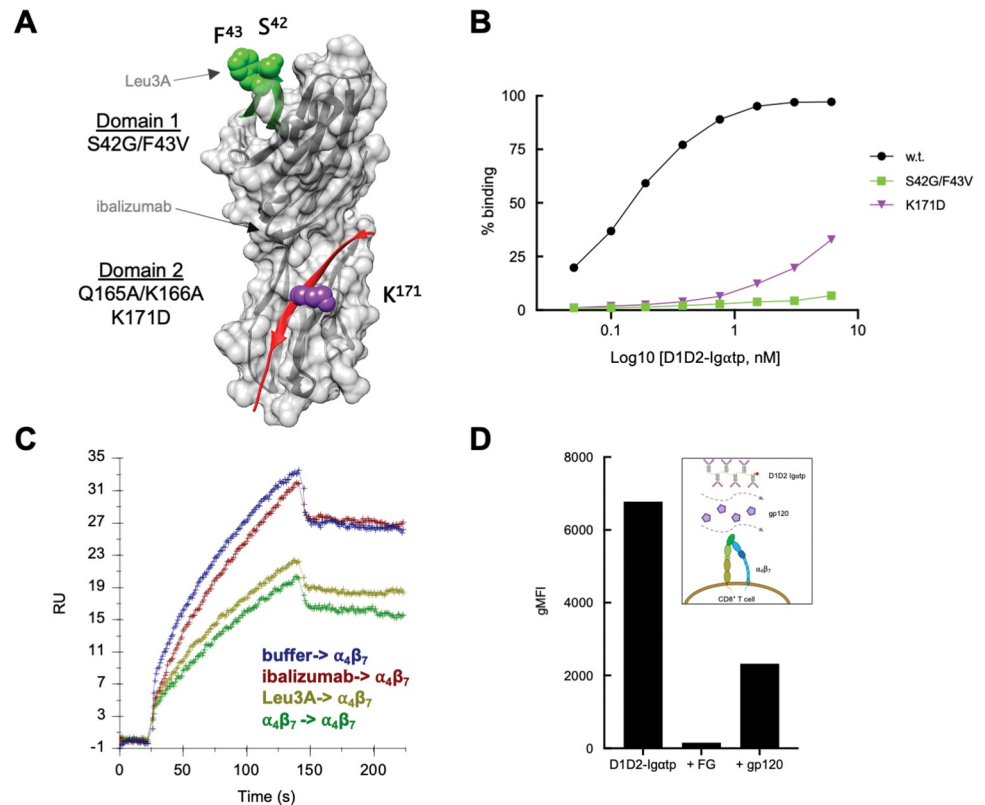


Fig 8. Mutating a gp120 contact site in CD4 D1 abrogates CD4- $\alpha_4\beta_7$ interactions. (A) Positions of amino acid substitutions introduced into D1D2-Ig α tp are indicated on a space-filling model of CD4 D1D2. Substitutions at S42/F43 in D1 (green) and K171 in D2 (purple) are shown. Approximate locations of mAb Leu3A and ibalizumab epitopes are indicated. (B) Flow-cytometric analysis of increasing amounts of D1D2-Ig α tp and mutant derivatives binding to $\alpha_4\beta_7$ on CD8⁺ T cells. Y-axis indicates % cells bound. (C) SPR analysis of soluble $\alpha_4\beta_7$ binding to a D1D2 coated surface following preincubation of the surface with ibalizumab (red), mAb Leu3A (light green), or $\alpha_4\beta_7$ (dark green). Y-axis indicates the mass of soluble $\alpha_4\beta_7$ bound at the end of the association phase. Mass of prebound inhibitors is subtracted. (D) Flow-cytometric analysis of unlabeled gp120 inhibiting PE labeled D1D2-Ig α tp binding to $\alpha_4\beta_7$ on CD8⁺ T cells. The integrin α_4 antagonist FG was employed as a control. Y-axis indicates MFI.

<https://doi.org/10.1371/journal.ppat.1011860.g008>

We next asked whether the CD4 D1 mAb Leu3A could block $\alpha_4\beta_7$ binding to CD4. Phe⁴³ is a key residue in the Leu3A epitope, and Leu3A is a potent neutralizing antibody that blocks gp120 binding to CD4 [57]. To this end, we employed an SPR-based kinetic binding assay in which soluble $\alpha_4\beta_7$ was passed over surface immobilized CD4 D1D2, in the presence vs absence of Leu3A. Leu3A reduced $\alpha_4\beta_7$ binding to the same degree as preloading (blocking) the surface with soluble $\alpha_4\beta_7$ (Fig 8C). Ibalizumab, a CD4 D2 mAb, which we employed as a reagent control, failed to inhibit $\alpha_4\beta_7$ binding. Taken together these results indicate that, in addition to the G β -strand of D2, a region of D1 including Phe⁴³ comprises a 2nd region of CD4 that mediates $\alpha_4\beta_7$ binding.

Finally, we asked whether gp120, CD4 and $\alpha_4\beta_7$ can form a ternary complex. Labeled D1D2-Ig α tp was bound to cell surface expressed $\alpha_4\beta_7$ in the presence vs absence of unlabeled gp120. With a 5X molar excess of gp120, we observed a >70% reduction in binding (Fig 8D). This finding is consistent with results presented in Fig 8B and suggests that binding sites on CD4, $\alpha_4\beta_7$ and gp120 utilize shared epitopes in a way that reduces the likelihood that all three proteins interact simultaneously.

We conclude that CD4, like MAdCAM-1 and VCAM-1 utilizes two sites to mediate $\alpha_4\beta_7$ interactions. Relative to MAdCAM-1 and VCAM-1, the two sites in CD4 are inverted, such

that the 1° CD4 binding site, as defined by the I/LD cation binding motif, lies in D2, while the accessory site lies in D1 (Fig 4B). This inversion may reflect a cis interaction in the case of CD4 vs. trans interactions for MAdCAM-1 and VCAM-1. The way that HIV has incorporated elements of this interaction into its envelope, summarized in S2B Fig, raises several questions, that are discussed below.

Discussion

In this study we identified a specific interaction between CD4, the HIV entry receptor, and $\alpha_4\beta_7$ an integrin that mediates lymphocyte trafficking to GALT. We found that the way these two receptors interact with each other is reflected in their individual interactions with HIV gp120. This finding supports the proposition that memory CD4⁺ T cells that co-express $\alpha_4\beta_7$ play a specific and important role in HIV pathogenesis [58,59].

We previously reported that, on CD4⁺ T cells, CD4 and $\alpha_4\beta_7$ can appear sufficiently close to each other to interact [36]. Here we report the results of two assays, one based on SPR measurements of $\alpha_4\beta_7$ binding to CD4 D1D2, and a second based on binding of oligomerized sCD4 to cell surface $\alpha_4\beta_7$, that provide clear evidence of a specific interaction between these two receptors. We do not exclude the possibility that CD4 interacts with $\alpha_4\beta_7$ in trans, however the combination of proximity and affinity argues for a cis interaction. It is well established that cis interactions between integrins and leukocyte receptors can regulate immune responses [37]. Several of these interactions involve receptors that, like CD4, present amino-terminal Ig-like domains [40,42]. The potential for $\alpha_4\beta_7$ to regulate CD4, or vice versa, is a subject worthy of future investigation, and may be relevant to efficacy of several α_4 integrin antagonists widely used in the treatment of IBDs and MS.

The selective pressures that underlie HIV evolving the capacity to bind to and signal through two receptors that interact with each other remain to be determined. Because $\alpha_4\beta_7$ adopts an active conformation only under certain conditions it is possible that $\alpha_4\beta_7$ provides a means for HIV to target cells that are susceptible to productive infection. This possibility is consistent with studies reporting the preferential infection of $\alpha_4\beta_7^{\text{high}}$ CD4⁺ T cells in vitro [36] and in vivo [33,60]. We know that $\alpha_4\beta_7$ is associated with migration to gut tissues, and thus gp120 affinity for $\alpha_4\beta_7$ could help explain the gut-tropic nature of HIV. Because CD4 migrates into the TCR in a transient way, where it plays an essential role in antigen recognition and the stabilization of immune synapses, we can speculate that interactions between CD4 and $\alpha_4\beta_7$ might regulate TCR activity. Perhaps HIV is exploiting this function to its own advantage. Finally, the close-proximity of $\alpha_4\beta_7$ to CD4 may impact viral entry and fusion. $\alpha_4\beta_7$ is not required for viral entry and cells lacking $\alpha_4\beta_7$ are clearly infected. However, productive infection is favored in activated cells, and gp120 delivers signals through $\alpha_4\beta_7$ [26,39]. Thus, engagement and signaling through $\alpha_4\beta_7$ either before or following CD4 binding may enhance infection in cells that are suboptimally activated. In this regard, integrins including $\alpha_4\beta_7$ mediate rearrangement of the cytoskeleton in the context of cellular activation [61].

Both MAdCAM-Ig and VCAM-Ig inhibit CD4 binding to $\alpha_4\beta_7$, indicating that CD4 engages the ligand binding groove in the $\alpha_4\beta_7$ headpiece. CD4- $\alpha_4\beta_7$ interactions could only be detected in the presence of Mn⁺⁺. Mn⁺⁺ drives the extension of the $\alpha_4\beta_7$ leg domains in a way that places the headpiece >20nm above the cell surface. The N-terminus of CD4 appears no more than 12 nm above the cell surface. How then could CD4 engage the $\alpha_4\beta_7$ headpiece in cis? We recognize two possibilities. Upon cellular activation, both the TCR and CD4 selectively migrate toward the raised tips of microvilli [62]. As such, the contours of a T cell could provide a way for an extended form of $\alpha_4\beta_7$ to engage CD4 when CD4 appears above the plane of the cell membrane. If in fact CD4- $\alpha_4\beta_7$ complexes are associated with specialized membrane

structures, this could explain the selective pressures that resulted in a gp120 that mimics CD4- $\alpha_4\beta_7$ interactions. Alternatively, some integrins headpieces can adopt an active conformation while their leg domains remain bent [49]. Current evidence indicates that the activated form of $\alpha_4\beta_7$ is extended [63], but perhaps the possibility of an additional form of $\alpha_4\beta_7$ that is activated but bent requires further investigation.

The structural similarities between CD4 D1D2, and the D1D2s of MAdCAM-1 and VCAM-1 suggest that CD4 might similarly utilize two sites (1° and accessory site) distributed across its two N-terminal domains to engage $\alpha_4\beta_7$. Peptides spanning residues 165–178 in D2, and 33–47 in D1 partially inhibited $\alpha_4\beta_7$ -CD4 interactions. Mutating residues in either of these two regions abrogated $\alpha_4\beta_7$ binding in the same way that substitutions in either the 1° or accessory sites of MAdCAM-1 and VCAM-1 also eliminate $\alpha_4\beta_7$ reactivity. Their 1° binding sites reside in their respective D1 domains, and each includes an essential Asp-aliphatic aa motif (MAdCAM-1: LD, VCAM-1: ID) that coordinates a divalent cation. An analogous motif (I¹⁷²D¹⁷³) appears in CD4 D2, and binding of a D2 peptide that includes these two residues is Mn⁺⁺-dependent. We therefore assigned CD4 residues 165–178 as the 1° $\alpha_4\beta_7$ binding site.

The sequence of the CD4 1° binding site is related to gp120 V2 aa 170–184, which mediates cation -dependent binding of gp120 V2 to $\alpha_4\beta_7$. 8 out of 14 CD4 1° binding site residues align with conserved residues in the V2 mid-region. Notably, the CD4 sequence KIDIV, is nearly identical to the conserved V2 sequence KLDIV. We show that a gp120 V2 peptide (pV2¹⁷⁰⁻¹⁸⁴) inhibits $\alpha_4\beta_7$ -CD4 interactions, while a CD4 D2 peptide (pCD4¹⁶⁵⁻¹⁷⁸) inhibits gp120 V2- $\alpha_4\beta_7$ interactions. This reciprocal pattern of inhibition is consistent with molecular mimicry.

MAdCAM-1 and VCAM-1 encode distinct accessory $\alpha_4\beta_7$ binding sites. Our findings indicate that the CD4 D1 C'C" strands and a connecting loop, also functions as an accessory binding site. Substituting residues Ser⁴² and Phe⁴³ with corresponding mouse residues eliminated $\alpha_4\beta_7$ reactivity. These substitutions do not disrupt the overall antigenic structure of D1 [57], and a high-resolution crystal structure of D1D2 with an F⁴³/V substitution found that this protein and w.t D1D2 were essentially isomorphous [64]. We conclude that the loss of $\alpha_4\beta_7$ reactivity mediated by these aa substitutions reflects a specific effect. Supporting this finding, mAb Leu3A, whose epitope includes Phe⁴³ [57], inhibits D1D2 binding to $\alpha_4\beta_7$. Whether CD4 D1 mediates CD4- $\alpha_4\beta_7$ interactions directly or indirectly is a subject of current investigation.

The sequence similarity between the $\alpha_4\beta_7$ binding sites in CD4 D2 and gp120 V2 is relevant to HIV vaccine development insofar as this region of V2 played a central role in RV144, the only HIV vaccine trial to achieve efficacy. Reduced risk in RV144 correlated with weakly-neutralizing antibodies specific to a region of V2 encompassed by aa 169–181 [65–67]. Moreover, V2 residues, K¹⁶⁹ and I¹⁸¹ were subject to vaccine -mediated immune pressure (sieving) in vaccinees who became infected [68]. I¹⁸¹ is included in the KIDIV sequence and K¹⁶⁹ is adjacent to Q¹⁷⁰K¹⁷¹. These observations indicate that the immune responses associated with reduced risk in RV144 target a region of gp120 V2 that mimics the 1° $\alpha_4\beta_7$ binding site in CD4 D2. Additionally, the primary contact sites of two RV144 -derived mAbs, CH58 and CH59, that are considered representative of the relevant RV144 Ab response lie within V2 aa 170–184 [69–71]. These mAbs block V2 adhesion to $\alpha_4\beta_7$ [29,56,71]. The prevailing view holds that reduced risk in RV144 was associated with V2 Ab effector functions [72]. We wonder whether the mechanistic explanations of RV144 reduced risk require further refinement. Such information may contribute to our understanding of the failure of HVTN702, a vaccine regimen intended to elicit V1V2 antibodies [73]. Overall, our findings provide an additional rationale for continuing to investigate the potential utility of V2 antibodies as part of an efficacious HIV vaccine.

The limitations of this study include a recognition that we do not know how the direct interaction between $\alpha_4\beta_7$ and CD4 impacts HIV infection. However, the presence of a

sequence in V2 that mimics CD4 D2 and shares with it the capacity to directly bind $\alpha_4\beta_7$ provides strong evidence that HIV is sensitive, in some way, to $\alpha_4\beta_7$ -CD4 interactions. This conclusion is consistent with the preferential infection in vivo of memory CD4⁺ T cells that co-express CD4 and $\alpha_4\beta_7$ [33]. Depending on whether CD4- $\alpha_4\beta_7$ interactions enhance or inhibit infection, it follows that circumstances that promote this interaction define a condition in which CD4⁺ T cells are either more or less susceptible to productive infection. Because productive infection is strongly impacted by the activation state of a cell, determining if and how CD4- $\alpha_4\beta_7$ interactions regulate CD4 participation in TCR-MHC II interactions may help resolve this question. Additionally, although not the subject of this study, our understanding of how gp120 interacts with $\alpha_4\beta_7$ is also incomplete, but relevant to the findings presented here. In contrast to the 1° $\alpha_4\beta_7$ binding site in CD4 D2, which is well exposed [10], the analogous $\alpha_4\beta_7$ binding site in gp120 V2 is partially hidden in the predominant ground state represented in prefusion trimers [13,74–78]. We do not know at which step in the transition of gp120 from the closed trimer to the open coreceptor bound state that V2 interacts with $\alpha_4\beta_7$, nor whether this interaction precedes or follows CD4 interactions with gp120. Perhaps a more detailed understanding of V2 conformation as the trimer moves away from its ground state will resolve the context in which gp120 engages $\alpha_4\beta_7$ [14,78].

In conclusion, in this report we identify two new aspects of the CD4 receptor and the way that it interacts with gp120 that are relevant to HIV pathogenesis. First, CD4 binds directly to $\alpha_4\beta_7$, the integrin most closely associated with T cell trafficking to GALT. Second, gp120 interactions with CD4 and $\alpha_4\beta_7$ reflect their interactions with each other. These findings underscore the view that $\alpha_4\beta_7$ -expressing CD4⁺ T cells play a specific and important role in HIV pathogenesis.

Materials and methods

Ethics statement

All primary T cells utilized in these studies were isolated from PBMCs, collected from healthy donors through a NIH Department of Transfusion Medicine protocol that was approved by the Institutional Review Board of the National Institute of Allergy and Infectious Diseases (NIAID), National Institutes of Health. Informed consent was written and was provided to study participants.

Cell line and reagents

RPMI8866 cells, a human B lymphoma cell line that constitutively expresses $\alpha_4\beta_7$ was purchased from Sigma-Aldrich. Cells were maintained in RPMI-1640 (Gibco) containing 10% heat inactivated fetal bovine serum (Gibco), 2% penicillin/streptomycin/glutamine (Gemini Bio-Products) and 0.1% all trans RA (Sigma). Cells were cultured for a minimum of 7 days prior to use. Primary CD4⁺ and CD8⁺ T cells were purified from buffy coats by negative bead selection. Cells were cultured in RPMI-1640 plus anti CD3, IL-2, and RA for a minimum of 8 days prior to use. CD4 D1D2 protein was a gift from Dr. E. Berger. Linear CD4 peptides and FAM conjugated peptides with > 90% purity were provided by Biopeptide. Cyclic V2 peptides were supplied by JPT Peptide Technologies. α_4 and β_7 expression vectors were purchased from Origene Technologies. Synthetic CD4 D1D2 and D1D2-Ig α tp genes were purchased from ATUM. Site directed mutagenesis was performed by Genscript. Transient transfections were carried out with Polyfect (Invitrogen), using standard protocols. CHO cell derived A244 gp120 (Lot 26539–1) was provided by Global Solutions for Infectious Diseases (San Francisco, CA). Purity was estimated at 97.1%. Vedolizumab was provided by the NIH Clinical Center Pharmacy Department. FG was purchased from MedChem Express. Human integrin α_4 mAb 2B4,

MAdCAM-Ig, VCAM-Ig and soluble $\alpha_4\beta_7$ were purchased from R&D Systems. Ibalizumab was generously provided by Dr. David Ho. Other mAbs were purchased from BD Biosciences. Dye labelling of D1D2-Ig $\alpha_4\beta_7$ was carried out using a LYNX HRP conjugation kit (Bio-Rad), following the manufacturer's instructions.

Flow cytometry binding assays

Cells were stained with fluoresceine conjugated mAbs or recombinant proteins using standard procedures preceded by Fc receptor blocking with human IgG. Buffers used were 10 mM HEPES 150 mM NaCl (HBS Buffer) with 100 μ M CaCl_2 . 1 mM MnCl_2 was also included, unless otherwise specified. Buffer without divalent cations included 0.1 mM EDTA. Unlabeled mAb or protein inhibitors were preincubated with cells or proteins at a 5X molar excess for 15 min on ice. FAM labeled peptides were used at 1.25 μ g/ 200,000 cells in a 100 μ l volume. Data were acquired using a FACSCanto II (BD Biosciences) and analyzed with FlowJo software (BD Biosciences). Plotted MFI values represent absolute values.

Surface plasmon resonance

Experiments were performed using a Biacore 3000 instrument (Cytiva Life Sciences) using CM4 or CM5 sensor chips. The data were evaluated using BIAevaluation 4.1.1 software (Cytiva Life Sciences). The chip surface was activated by injecting 35 μ l of a 1:1 mixture of 0.05 M *N*-hydroxysuccinimide and 0.2 M *N*-ethyl-*N*-(dimethylaminopropyl) carbodiimide at 5 μ l/min. NeutrAvidin, HIV gp120, sCD4 (D1D2) or Hu-MAdCAM-Ig (R&D Systems) at concentrations of 5 μ g/ml in 10mM NaOAc, pH 4.5, were immobilized to 250–750 resonance units (RU). After the proteins were immobilized to the desired densities, unreacted sites were blocked with 35 μ l of 1 M Tris-HCl (pH 8.0). Biotinylated cyclic V2 peptides (1 μ g/ml in 20 mM Tris-HCl, pH 8.0) were bound to the NeutrAvidin surfaces to densities of approximately 250–300 RU. One surface was activated and blocked without ligand as a control surface for non-specific binding. Signal from the control surface was subsequently subtracted. Running buffer was HBS (pH 7.4), 1 mM MnCl_2 , 0.005% Tween- 20, 0.05% soluble carboxymethyl-dextran. Binding experiments were carried out at a flow rate of 25 μ l/min at 25°C. After a 2 min injection, the surface was washed for an additional 2 min in running buffer allowing dissociation of the bound ligand from the surface. The surfaces were regenerated by multiple injections of 4.5 M MgCl_2 at a flow rate of 100 μ l/min. Inhibition of $\alpha_4\beta_7$ binding by linear V2-loop and CD4 derived peptides was carried out by pre-incubating $\alpha_4\beta_7$ with the peptides in running buffer at the indicated concentrations for 2 hours at room temperature prior to passing them over the prepared surfaces as described above. Cross-inhibition experiments were performed by passing either buffer or the listed analytes over a surface to which sCD4 (D1D2) had been immobilized, followed by a secondary sequential injection of $\alpha_4\beta_7$. The ability of each analyte to inhibit either itself or $\alpha_4\beta_7$ was determined by comparing the binding of $\alpha_4\beta_7$ in the absence or presence of the listed pre-bound analytes as previously described [79]. Illustration of the dynamic range of range of linear peptide inhibition assays is provided in S4 Fig.

FRET/FLIM

Primary CD4⁺ T cells were cultured in IL-2 + anti CD3 + RA (10nM) for a minimum of 10 days. RA -mediated upregulation of $\alpha_4\beta_7$ was verified by flow cytometry prior to mAb staining and FRET\FLIM Imaging. FLIM sample staining was carried out 2 days after fresh media exchange. Samples were reacted with the following antibodies using standard immunofluorescence methods. Donor mAbs (AF488 conjugated) includes OKT4 (BioLegend 317420), FIB504 (lab conjugated), Leu3A (Biolegend 344618). Acceptor mAbs (AF546 conjugated)

includes FIB504 (lab conjugated), OKT4 (lab conjugated). Mock and gp120 treatments were performed in the same volume of PBS (cells: 2×10^6 /mL), for 20 or 60 min at 37°C in the dark, in the presence of 5% CO₂. Treatments were stopped by 4 vigorous washes in high volumes (3x) of ice-cold complete media, followed by 1 wash in PBS + BSA, then fixed in 2% MeOH-free PFA at 4°C. After the completion of the staining procedure (~16 hrs) samples were cytospun onto imaging slides at 400 rpm for 6 min. Slides were then mounted with imaging coverslips using prolong gold mounting media with antifade-no DAPI (Invitrogen) and cured thoroughly in the dark at room temperature before imaging. Images were acquired using a Leica DMI6000 confocal microscope coupled with Becker and Hickel Lifetime measurement module. Data were collected in excess of 1000 photons per pixel to fit the curve in a multi-modal decay plot. Images were post-processed using ImageJ/NIHimage analysis software.

Proximity ligation assay

Flow cytometry based PLA assays (Sigma Aldrich) were carried out per the manufacturer's instructions. In brief, an oligonucleotide conjugated anti CD4 mAb (clone DB81) (plus strand) and an oligonucleotide conjugated anti integrin β_7 mAb (clone FIB27) (minus strand) were generated using a Duolink In Situ Probemaker kit. Freshly isolated purified CD4⁺ T cells were fixed in 1% PFA and blocked with buffer containing 2% donkey serum, 10% BSA and 0.2% gelatin. Cells were incubated with mAb probes for 30 min at 37°C in buffer containing 0.2% donkey serum, 10% BSA and 0.2% gelatin. Additional fluorescein based mAbs (vedolizumab and CD45RA) were included. After washing, cells were treated with DNA ligase and Duolink ligation buffer for 30 min at 37°C. After washing, cells were treated with Duolink amplification buffer and DNA polymerase O/N at 37°C. Cells were washed and treated with Duolink detection buffer (Far Red) for 30 min at 37°C. After washing cells were resuspended in PBS and analyzed by flow-cytometry. All washes were carried in Duolink wash buffer.

CD4 and gp120 V2 sequence alignments and analysis

All gp120 aa sequences were numbered based on HXB2. Frequencies of gp120 V2 aa were established by accessing the HIV ENV web alignment from Los Alamos database (<https://www.hiv.lanl.gov/content/sequence/NEWALIGN/align.html> (accession date 09/29/2022)). Sequences from different HIV subtypes and recombinants were utilized and represent the full spectrum of HIV envelope sequences from the LANL database. All non-group M sequences were excluded from this analysis. Geneious 11.1.5 software was used to determine the frequencies of I, L and V at gp120 position 181. HIV ENV web alignment was used to generate the logo figure on WebLogo3 software (DOI: [10.1101/gr.849004](https://doi.org/10.1101/gr.849004)). Protein motifs were scanned against the Swiss-Prot database using the Prosite tool (doi:[10.1093/nar/gks1067](https://doi.org/10.1093/nar/gks1067), <https://doi.org/10.1093/nar/gkl124>).

Data and materials availability

All data are available in the main text or the supplementary materials.

Supporting information

S1 Fig. Dynamic association of CD4 and $\alpha_4\beta_7$ on $\alpha_4\beta_7^{\text{high}}$ CD4⁺ T cells. (A) Schematic of trans vs cis interactions of integrins with counter receptors. (B) PLA assay for CD4 and Integrin β_7 with PLA antibody probes (CD4 mAb (plus strand) and β_7 mAb (minus strand)). Representative flow cytometric dot plot of freshly isolated primary CD4⁺ T cells stained with vedolizumab (Y-axis) and CD45RA (X-axis). $\alpha_4\beta_7^{\text{high}}$ (yellow), $\alpha_4\beta_7^{\text{int}}$ (blue), and $\alpha_4\beta_7^{\text{low}}$ (green) gates are shown, with cell population frequencies depicted (middle). Pie charts (right)

indicate the frequency of PLA positive cells (red) within the $\alpha_4\beta_7^{\text{high}}$, $\alpha_4\beta_7^{\text{int}}$, and $\alpha_4\beta_7^{\text{low}}$ gates. (C) FLIM analysis of $\alpha_4\beta_7^{\text{high}}$ CD4⁺ T cells stained with dye labeled anti CD4 (donor) and anti β_7 (acceptor) mAbs. Cells mock treated and stained with CD4 mAb alone (green). Cells stained with CD4 and β_7 mAbs following mock treatment (black), gp120 treated for 20 min (blue), or gp120 treated for 60 min (red). Number of cells analyzed as indicated. Y-axis and X-axis indicate normalized frequency and lifetime (picoseconds) respectively. (D) Representative images of cells stained with CD4 alone (left), CD4 and β_7 mAbs following mock treatment (center), or CD4 and β_7 mAbs following 60 min gp120 treatment (right). Color bar represents heatmap for the interaction in picoseconds.

(TIF)

S2 Fig. Potential regulatory role of a CD4- $\alpha_4\beta_7$ cis interaction. (A) Cis interaction between CD4 D1D2 and the headpiece domain of $\alpha_4\beta_7$. (B) Schematic summarizing the interactions of CD4 with gp120 and $\alpha_4\beta_7$.

(TIF)

S3 Fig. CD4 D2 aa 165–178 sequence conservation in nonhuman primates. Amino acids 165–178 in nonhuman primate CD4 orthologs. Residues that align with conserved gp120 V2 residues 170–184 are shaded in grey.

(TIF)

S4 Fig. Linear peptide inhibition of D1D2- $\alpha_4\beta_7$ interactions by SPR. Recombinant $\alpha_4\beta_7$ (analyte) reacted with surface bound CD4 D1D2 in the absence or presence of increasing concentrations of peptide pCD4¹⁶⁵⁻¹⁷⁵. Y-axis indicates relative mass units (RU) (left). Peak RU at the termination of the association phase (150s), plotted against peptide concentration (right).

(TIF)

S5 Fig. Inhibition of D1D2- $\alpha_4\beta_7$ interactions by New- and Old-World monkey CD4 peptides. SPR assays of recombinant $\alpha_4\beta_7$ (analyte) reacted with surface bound CD4 D1D2 in the absence or presence of increasing concentrations of Gorilla (left) and Aotus (right) analogs of peptide pCD4¹⁶⁵⁻¹⁷⁵. Y-axis indicates relative mass units (RU) (upper). Amino acid sequence alignment of Gorilla and Aotus pCD4¹⁶⁵⁻¹⁷⁵ analogs (lower). Dots indicate identity.

(TIF)

S1 Table. $\alpha_4\beta_7$ binding kinetics.

(DOCX)

S2 Table. CD4 peptides amino acids +1(23)-188*.

(DOCX)

S3 Table. Proteins encoding CD4 1° binding site motifs.

(DOCX)

Acknowledgments

The authors would like to thank Dr. David Ho for ibalizumab, and Dr. Edward Berger for CD4 D1D2. Drs. Luca Schifanella, Aftab Ansari, Fatima Nawaz, and Genoveffa Franchini for critical review of the manuscript.

Disclaimer

Material has been reviewed by the Walter Reed Army Institute of Research. There is no objection to its presentation and/or publication. The opinions or assertions contained herein are

the private views of the author, and are not to be construed as official, or as reflecting true views of the Department of the Army or the Department of Defense. The investigators have adhered to the policies for protection of human subjects as prescribed in AR 70–25.

Author Contributions

Conceptualization: Donald Van Ryk, Sinmanus Vimompatranon, Sundar Ganesan, Marcelo A. Soares, Elena Martinelli, Claudia Cicala, James Arthos.

Formal analysis: Danlan Wei, Dawei Huang.

Investigation: Donald Van Ryk, Sinmanus Vimompatranon, Joe Hiatt, Sundar Ganesan, Nathalie Chen, Jordan McMurry, Saadiq Garba, Susie Min, Livia R. Goes, Alexandre Girard, Jason Yolitz, Isabella Licavoli, Danlan Wei.

Methodology: Donald Van Ryk, Sinmanus Vimompatranon, Joe Hiatt, Alexandre Girard, Danlan Wei, Dawei Huang.

Project administration: James Arthos.

Supervision: Sinmanus Vimompatranon, Marcelo A. Soares, Claudia Cicala, James Arthos.

Validation: Donald Van Ryk, Claudia Cicala, James Arthos.

Visualization: Sinmanus Vimompatranon, Sundar Ganesan, Alexandre Girard.

Writing – original draft: James Arthos.

Writing – review & editing: Donald Van Ryk, Sinmanus Vimompatranon, Sundar Ganesan, Danlan Wei, Dawei Huang, Elena Martinelli, Claudia Cicala, James Arthos.

References

1. Dalgleish AG, Beverley PC, Clapham PR, Crawford DH, Greaves MF, Weiss RA. The CD4 (T4) antigen is an essential component of the receptor for the AIDS retrovirus. *Nature*. 1984; 312(5996):763–7. <https://doi.org/10.1038/312763a0> PMID: 6096719.
2. Klatzmann D, Champagne E, Chamaret S, Gruest J, Guetard D, Hercend T, et al. T-lymphocyte T4 molecule behaves as the receptor for human retrovirus LAV. *Nature*. 1984; 312(5996):767–8. <https://doi.org/10.1038/312767a0> PMID: 6083454.
3. Maddon PJ, Dalgleish AG, McDougal JS, Clapham PR, Weiss RA, Axel R. The T4 gene encodes the AIDS virus receptor and is expressed in the immune system and the brain. *Cell*. 1986; 47(3):333–48. [https://doi.org/10.1016/0092-8674\(86\)90590-8](https://doi.org/10.1016/0092-8674(86)90590-8) PMID: 3094962.
4. Lasky LA, Groopman JE, Fennie CW, Benz PM, Capon DJ, Dowbenko DJ, et al. Neutralization of the AIDS retrovirus by antibodies to a recombinant envelope glycoprotein. *Science*. 1986; 233(4760):209–12. <https://doi.org/10.1126/science.3014647> PMID: 3014647.
5. Myszka DG, Sweet RW, Hensley P, Brigham-Burke M, Kwong PD, Hendrickson WA, et al. Energetics of the HIV gp120-CD4 binding reaction. *Proc Natl Acad Sci U S A*. 2000; 97(16):9026–31. <https://doi.org/10.1073/pnas.97.16.9026> PMID: 10922058; PubMed Central PMCID: PMC16815.
6. Kwong PD, Doyle ML, Casper DJ, Cicala C, Leavitt SA, Majeed S, et al. HIV-1 evades antibody-mediated neutralization through conformational masking of receptor-binding sites. *Nature*. 2002; 420(6916):678–82. <https://doi.org/10.1038/nature01188> PMID: 12478295.
7. Maddon PJ, Littman DR, Godfrey M, Maddon DE, Chess L, Axel R. The isolation and nucleotide sequence of a cDNA encoding the T cell surface protein T4: a new member of the immunoglobulin gene family. *Cell*. 1985; 42(1):93–104. [https://doi.org/10.1016/s0092-8674\(85\)80105-7](https://doi.org/10.1016/s0092-8674(85)80105-7) PMID: 2990730.
8. Arthos J, Deen KC, Chaikin MA, Fornwald JA, Sathe G, Sattentau QJ, et al. Identification of the residues in human CD4 critical for the binding of HIV. *Cell*. 1989; 57(3):469–81. [https://doi.org/10.1016/0092-8674\(89\)90922-7](https://doi.org/10.1016/0092-8674(89)90922-7) PMID: 2541915.
9. Kwong PD, Wyatt R, Robinson J, Sweet RW, Sodroski J, Hendrickson WA. Structure of an HIV gp120 envelope glycoprotein in complex with the CD4 receptor and a neutralizing human antibody. *Nature*.

- 1998; 393(6686):648–59. <https://doi.org/10.1038/31405> PMID: 9641677; PubMed Central PMCID: PMC5629912.
10. Ryu SE, Kwong PD, Truneh A, Porter TG, Arthos J, Rosenberg M, et al. Crystal structure of an HIV-binding recombinant fragment of human CD4. *Nature*. 1990; 348(6300):419–26. <https://doi.org/10.1038/348419a0> PMID: 2247146; PubMed Central PMCID: PMC5638305.
 11. Sattentau QJ, Moore JP. Conformational changes induced in the human immunodeficiency virus envelope glycoprotein by soluble CD4 binding. *J Exp Med*. 1991; 174(2):407–15. <https://doi.org/10.1084/jem.174.2.407> PMID: 1713252; PubMed Central PMCID: PMC2118908.
 12. Wyatt R, Sodroski J. The HIV-1 envelope glycoproteins: fusogens, antigens, and immunogens. *Science*. 1998; 280(5371):1884–8. <https://doi.org/10.1126/science.280.5371.1884> PMID: 9632381.
 13. Munro JB, Gorman J, Ma X, Zhou Z, Arthos J, Burton DR, et al. Conformational dynamics of single HIV-1 envelope trimers on the surface of native virions. *Science*. 2014; 346(6210):759–63. Epub 20141008. <https://doi.org/10.1126/science.1254426> PMID: 25298114; PubMed Central PMCID: PMC4304640.
 14. Wang H, Barnes CO, Yang Z, Nussenzweig MC, Bjorkman PJ. Partially Open HIV-1 Envelope Structures Exhibit Conformational Changes Relevant for Coreceptor Binding and Fusion. *Cell Host Microbe*. 2018; 24(4):579–92 e4. <https://doi.org/10.1016/j.chom.2018.09.003> PMID: 30308160; PubMed Central PMCID: PMC6185872.
 15. Feng Y, Broder CC, Kennedy PE, Berger EA. HIV-1 entry cofactor: functional cDNA cloning of a seven-transmembrane, G protein-coupled receptor. *Science*. 1996; 272(5263):872–7. <https://doi.org/10.1126/science.272.5263.872> PMID: 8629022.
 16. Ward AB, Wilson IA. The HIV-1 envelope glycoprotein structure: nailing down a moving target. *Immunol Rev*. 2017; 275(1):21–32. <https://doi.org/10.1111/imr.12507> PMID: 28133813; PubMed Central PMCID: PMC5300090.
 17. Doyle C, Strominger JL. Interaction between CD4 and class II MHC molecules mediates cell adhesion. *Nature*. 1987; 330(6145):256–9. <https://doi.org/10.1038/330256a0> PMID: 2823150.
 18. Janeway CA Jr., The T cell receptor as a multicomponent signalling machine: CD4/CD8 coreceptors and CD45 in T cell activation. *Annu Rev Immunol*. 1992; 10:645–74. <https://doi.org/10.1146/annurev.iy.10.040192.003241> PMID: 1534242.
 19. Veillette A, Bookman MA, Horak EM, Samelson LE, Bolen JB. Signal transduction through the CD4 receptor involves the activation of the internal membrane tyrosine-protein kinase p56lck. *Nature*. 1989; 338(6212):257–9. <https://doi.org/10.1038/338257a0> PMID: 2784195.
 20. Sweet RW, Truneh A, Hendrickson WA. CD4: its structure, role in immune function and AIDS pathogenesis, and potential as a pharmacological target. *Curr Opin Biotechnol*. 1991; 2(4):622–33. [https://doi.org/10.1016/0958-1669\(91\)90089-n](https://doi.org/10.1016/0958-1669(91)90089-n) PMID: 1367682.
 21. Fleury S, Lamarre D, Meloche S, Ryu SE, Cantin C, Hendrickson WA, et al. Mutational analysis of the interaction between CD4 and class II MHC: class II antigens contact CD4 on a surface opposite the gp120-binding site. *Cell*. 1991; 66(5):1037–49. [https://doi.org/10.1016/0092-8674\(91\)90447-7](https://doi.org/10.1016/0092-8674(91)90447-7) PMID: 1889086.
 22. Huang B, Yachou A, Fleury S, Hendrickson WA, Sekaly RP. Analysis of the contact sites on the CD4 molecule with class II MHC molecule: co-ligand versus co-receptor function. *J Immunol*. 1997; 158(1):216–25. PMID: 8977193.
 23. Geijtenbeek TB, Kwon DS, Torensma R, van Vliet SJ, van Duynhoven GC, Middel J, et al. DC-SIGN, a dendritic cell-specific HIV-1-binding protein that enhances trans-infection of T cells. *Cell*. 2000; 100(5):587–97. [https://doi.org/10.1016/s0092-8674\(00\)80694-7](https://doi.org/10.1016/s0092-8674(00)80694-7) PMID: 10721995.
 24. Zou Z, Chastain A, Moir S, Ford J, Trandem K, Martinelli E, et al. Siglecs facilitate HIV-1 infection of macrophages through adhesion with viral sialic acids. *PLoS One*. 2011; 6(9):e24559. Epub 20110908. <https://doi.org/10.1371/journal.pone.0024559> PMID: 21931755; PubMed Central PMCID: PMC3169630.
 25. Turville SG, Cameron PU, Handley A, Lin G, Pohlmann S, Doms RW, et al. Diversity of receptors binding HIV on dendritic cell subsets. *Nat Immunol*. 2002; 3(10):975–83. Epub 20020923. <https://doi.org/10.1038/ni841> PMID: 12352970.
 26. Arthos J, Cicala C, Martinelli E, Macleod K, Van Ryk D, Wei D, et al. HIV-1 envelope protein binds to and signals through integrin $\alpha_4\beta_7$, the gut mucosal homing receptor for peripheral T cells. *Nat Immunol*. 2008; 9(3):301–9. Epub 2008/02/12. <https://doi.org/10.1038/ni1566> PMID: 18264102.
 27. Nakamura GR, Fonseca DP, O'Rourke SM, Vollrath AL, Berman PW. Monoclonal antibodies to the V2 domain of MN-rgp120: fine mapping of epitopes and inhibition of $\alpha_4\beta_7$ binding. *PLoS One*. 2012; 7(6):e39045. Epub 20120613. <https://doi.org/10.1371/journal.pone.0039045> PMID: 22720026; PubMed Central PMCID: PMC3374778.

28. Tassaneeritthep B, Tivon D, Swetnam J, Karasavvas N, Michael NL, Kim JH, et al. Cryptic determinant of alpha4beta7 binding in the V2 loop of HIV-1 gp120. *PLoS One*. 2014; 9(9):e108446. Epub 20140929. <https://doi.org/10.1371/journal.pone.0108446> PMID: 25265384; PubMed Central PMCID: PMC4180765.
29. Peachman KK, Karasavvas N, Chenine AL, McLinden R, Rerks-Ngarm S, Jaranit K, et al. Identification of New Regions in HIV-1 gp120 Variable 2 and 3 Loops that Bind to alpha4beta7 Integrin Receptor. *PLoS One*. 2015; 10(12):e0143895. Epub 20151201. <https://doi.org/10.1371/journal.pone.0143895> PMID: 26625359; PubMed Central PMCID: PMC4666614.
30. Berlin C, Berg EL, Briskin MJ, Andrew DP, Kilshaw PJ, Holzmann B, et al. Alpha 4 beta 7 integrin mediates lymphocyte binding to the mucosal vascular addressin MAdCAM-1. *Cell*. 1993; 74(1):185–95. [https://doi.org/10.1016/0092-8674\(93\)90305-a](https://doi.org/10.1016/0092-8674(93)90305-a) PMID: 7687523.
31. Wagner N, Lohler J, Kunkel EJ, Ley K, Leung E, Krissansen G, et al. Critical role for beta7 integrins in formation of the gut-associated lymphoid tissue. *Nature*. 1996; 382(6589):366–70. <https://doi.org/10.1038/382366a0> PMID: 8684468.
32. Sivro A, Schuetz A, Sheward D, Joag V, Yegorov S, Liebenberg LJ, et al. Integrin alpha4beta7 expression on peripheral blood CD4(+) T cells predicts HIV acquisition and disease progression outcomes. *Sci Transl Med*. 2018; 10(425). <https://doi.org/10.1126/scitranslmed.aam6354> PMID: 29367348; PubMed Central PMCID: PMC6820005.
33. Tokarev A, McKinnon LR, Pagliuzza A, Sivro A, Omole TE, Kroon E, et al. Preferential Infection of alpha4beta7+ Memory CD4+ T Cells During Early Acute Human Immunodeficiency Virus Type 1 Infection. *Clin Infect Dis*. 2020; 71(11):e735–e43. <https://doi.org/10.1093/cid/ciaa497> PMID: 32348459; PubMed Central PMCID: PMC7778353.
34. Kader M, Wang X, Piatak M, Lifson J, Roederer M, Veazey R, et al. Alpha4(+)beta7(hi)CD4(+) memory T cells harbor most Th-17 cells and are preferentially infected during acute SIV infection. *Mucosal Immunol*. 2009; 2(5):439–49. Epub 2009/07/03. <https://doi.org/10.1038/mi.2009.90> PMID: 19571800; PubMed Central PMCID: PMC2763371.
35. Byrareddy SN, Kallam B, Arthos J, Cicala C, Nawaz F, Hiatt J, et al. Targeting alpha4beta7 integrin reduces mucosal transmission of simian immunodeficiency virus and protects gut-associated lymphoid tissue from infection. *Nat Med*. 2014; 20(12):1397–400. Epub 2014/11/25. <https://doi.org/10.1038/nm.3715> PMID: 25419708; PubMed Central PMCID: PMC4257865.
36. Cicala C, Martinelli E, McNally JP, Goode DJ, Gopaul R, Hiatt J, et al. The integrin alpha4beta7 forms a complex with cell-surface CD4 and defines a T-cell subset that is highly susceptible to infection by HIV-1. *Proc Natl Acad Sci U S A*. 2009; 106(49):20877–82. Epub 2009/11/26. <https://doi.org/10.1073/pnas.0911796106> PMID: 19933330; PubMed Central PMCID: PMC2780317.
37. Porter JC, Hogg N. Integrins take partners: cross-talk between integrins and other membrane receptors. *Trends Cell Biol*. 1998; 8(10):390–6. [https://doi.org/10.1016/s0962-8924\(98\)01344-0](https://doi.org/10.1016/s0962-8924(98)01344-0) PMID: 9789327.
38. Nawaz F, Goes LR, Ray JC, Olowojesiku R, Sajani A, Ansari AA, et al. MAdCAM costimulation through Integrin-alpha4beta7 promotes HIV replication. *Mucosal Immunol*. 2018. Epub 2018/06/08. <https://doi.org/10.1038/s41385-018-0044-1> PMID: 29875402.
39. Goes LR, Sajani A, Sivro A, Olowojesiku R, Ray JC, Perrone I, et al. The V2 loop of HIV gp120 delivers costimulatory signals to CD4(+) T cells through Integrin alpha4beta7 and promotes cellular activation and infection. *Proc Natl Acad Sci U S A*. 2020; 117(51):32566–73. Epub 20201207. <https://doi.org/10.1073/pnas.2011501117> PubMed Central PMCID: PMC7768698.
40. Saggi G, Okubo K, Chen Y, Vattepu R, Tsuboi N, Rosetti F, et al. Cis interaction between sialylated FcgammaRIIA and the alpha-domain of Mac-1 limits antibody-mediated neutrophil recruitment. *Nat Commun*. 2018; 9(1):5058. Epub 20181129. <https://doi.org/10.1038/s41467-018-07506-1> PMID: 30498196; PubMed Central PMCID: PMC6265255.
41. Brummer J, Ebrahimnejad A, Flayeh R, Schumacher U, Loning T, Bamberger AM, et al. cis Interaction of the cell adhesion molecule CEACAM1 with integrin beta(3). *Am J Pathol*. 2001; 159(2):537–46. [https://doi.org/10.1016/s0002-9440\(10\)61725-7](https://doi.org/10.1016/s0002-9440(10)61725-7) PMID: 11485912; PubMed Central PMCID: PMC1850541.
42. Fan Z, McArdle S, Marki A, Mikulski Z, Gutierrez E, Engelhardt B, et al. Neutrophil recruitment limited by high-affinity bent beta2 integrin binding ligand in cis. *Nat Commun*. 2016; 7:12658. Epub 20160831. <https://doi.org/10.1038/ncomms12658> PMID: 27578049; PubMed Central PMCID: PMC5013657.
43. Wang XQ, Frazier WA. The thrombospondin receptor CD47 (IAP) modulates and associates with alpha2 beta1 integrin in vascular smooth muscle cells. *Mol Biol Cell*. 1998; 9(4):865–74. <https://doi.org/10.1091/mbc.9.4.865> PMID: 9529384; PubMed Central PMCID: PMC25313.
44. Lindberg FP, Gresham HD, Reinhold MI, Brown EJ. Integrin-associated protein immunoglobulin domain is necessary for efficient vitronectin bead binding. *J Cell Biol*. 1996; 134(5):1313–22. <https://doi.org/10.1083/jcb.134.5.1313> PMID: 8794870; PubMed Central PMCID: PMC2120984.

45. Arthos J, Cicala C, Steenbeke TD, Chun TW, Dela Cruz C, Hanback DB, et al. Biochemical and biological characterization of a dodecameric CD4-Ig fusion protein: implications for therapeutic and vaccine strategies. *J Biol Chem.* 2002; 277(13):11456–64. Epub 20020122. <https://doi.org/10.1074/jbc.M111191200> PMID: 11805109.
46. Miller DH, Weber T, Grove R, Wardell C, Horrigan J, Graff O, et al. Fingertegrast for relapsing remitting multiple sclerosis: a phase 2, randomised, double-blind, placebo-controlled trial. *Lancet Neurol.* 2012; 11(2):131–9. Epub 20120105. [https://doi.org/10.1016/S1474-4422\(11\)70299-X](https://doi.org/10.1016/S1474-4422(11)70299-X) PMID: 22226929.
47. Karimi F O'Connor AJ, Qiao GG, Heath DE. Integrin Clustering Matters: A Review of Biomaterials Functionalized with Multivalent Integrin-Binding Ligands to Improve Cell Adhesion, Migration, Differentiation, Angiogenesis, and Biomedical Device Integration. *Adv Healthc Mater.* 2018; 7(12):e1701324. Epub 20180325. <https://doi.org/10.1002/adhm.201701324> PMID: 29577678.
48. Wang S, Wu C, Zhang Y, Zhong Q, Sun H, Cao W, et al. Integrin $\alpha_4\beta_7$ switches its ligand specificity via distinct conformer-specific activation. *J Cell Biol.* 2018; 217(8):2799–812. Epub 20180522. <https://doi.org/10.1083/jcb.201710022> PMID: 29789438; PubMed Central PMCID: PMC6080939.
49. Arnaout MA, Mahalingam B, Xiong JP. Integrin structure, allostery, and bidirectional signaling. *Annu Rev Cell Dev Biol.* 2005; 21:381–410. <https://doi.org/10.1146/annurev.cellbio.21.090704.151217> PMID: 16212500.
50. Feagan BG, Greenberg GR, Wild G, Fedorak RN, Pare P, McDonald JW, et al. Treatment of active Crohn's disease with MLN0002, a humanized antibody to the $\alpha_4\beta_7$ integrin. *Clin Gastroenterol Hepatol.* 2008; 6(12):1370–7. Epub 20081001. <https://doi.org/10.1016/j.cgh.2008.06.007> PMID: 18829392.
51. Stefanich EG, Danilenko DM, Wang H, O'Byrne S, Erickson R, Gelzleichter T, et al. A humanized monoclonal antibody targeting the β_7 integrin selectively blocks intestinal homing of T lymphocytes. *Br J Pharmacol.* 2011; 162(8):1855–70. <https://doi.org/10.1111/j.1476-5381.2011.01205.x> PMID: 21232034; PubMed Central PMCID: PMC3081127.
52. Sheremata WA, Vollmer TL, Stone LA, Willmer-Hulme AJ, Koller M. A safety and pharmacokinetic study of intravenous natalizumab in patients with MS. *Neurology.* 1999; 52(5):1072–4. <https://doi.org/10.1212/wnl.52.5.1072> PMID: 10102433.
53. Newham P, Craig SE, Seddon GN, Schofield NR, Rees A, Edwards RM, et al. α_4 integrin binding interfaces on VCAM-1 and MAdCAM-1. Integrin binding footprints identify accessory binding sites that play a role in integrin specificity. *J Biol Chem.* 1997; 272(31):19429–40. <https://doi.org/10.1074/jbc.272.31.19429> PMID: 9235944.
54. Green N, Rosebrook J, Cochran N, Tan K, Wang JH, Springer TA, et al. Mutational analysis of MAdCAM-1/ $\alpha_4\beta_7$ interactions reveals significant binding determinants in both the first and second immunoglobulin domains. *Cell Adhes Commun.* 1999; 7(3):167–81. <https://doi.org/10.3109/15419069909010800> PMID: 10626902.
55. Chand S, Messina EL, AlSalmi W, Ananthaswamy N, Gao G, Uritskiy G, et al. Glycosylation and oligomeric state of envelope protein might influence HIV-1 virion capture by $\alpha_4\beta_7$ integrin. *Virology.* 2017; 508:199–212. Epub 20170531. <https://doi.org/10.1016/j.virol.2017.05.016> PMID: 28577856; PubMed Central PMCID: PMC5526109.
56. Lertjuthaporn S, Cicala C, Van Ryk D, Liu M, Yolitz J, Wei D, et al. Select gp120 V2 domain specific antibodies derived from HIV and SIV infection and vaccination inhibit gp120 binding to $\alpha_4\beta_7$. *PLoS Pathog.* 2018; 14(8):e1007278. Epub 2018/08/29. <https://doi.org/10.1371/journal.ppat.1007278> PMID: 30153309; PubMed Central PMCID: PMC6130882 following competing interests: JA, CC and ASF are inventors of patent 20160075786 submitted by the NIAID, NIH that covers the study of reagents that serve as antagonists of the interaction between HIV gp120 and $\alpha_4\beta_7$ mAb. The funders had no role in study design, data collection and analysis, decision to publish, or preparation of the manuscript.
57. Sattentau QJ, Arthos J, Deen K, Hanna N, Healey D, Beverley PC, et al. Structural analysis of the human immunodeficiency virus-binding domain of CD4. Epitope mapping with site-directed mutants and anti-idiotypes. *J Exp Med.* 1989; 170(4):1319–34. <https://doi.org/10.1084/jem.170.4.1319> PMID: 2477490; PubMed Central PMCID: PMC2189462.
58. Cicala C, Arthos J, Fauci AS. HIV-1 envelope, integrins and co-receptor use in mucosal transmission of HIV. *J Transl Med.* 2011; 9 Suppl 1(Suppl 1):S2. Epub 20110127. <https://doi.org/10.1186/1479-5876-9-S1-S2> PMID: 21284901; PubMed Central PMCID: PMC3105502.
59. Cicala C, Arthos J, Fauci AS. Role of T-cell trafficking in the pathogenesis of HIV disease. *Curr Opin HIV AIDS.* 2019; 14(2):115–20. <https://doi.org/10.1097/COH.0000000000000529> PMID: 30601238.
60. Kader M, Bixler S, Roederer M, Veazey R, Mattapallil JJ. CD4 T cell subsets in the mucosa are CD28 + Ki-67-HLA-DR-CD69+ but show differential infection based on $\alpha_4\beta_7$ receptor expression during acute SIV infection. *J Med Primatol.* 2009; 38 Suppl 1:24–31. Epub 2009/10/30. <https://doi.org/10.1111/j.1600-0684.2009.00372.x> PMID: 19863675; PubMed Central PMCID: PMC2813512.

61. Springer TA, Dustin ML. Integrin inside-out signaling and the immunological synapse. *Curr Opin Cell Biol.* 2012; 24(1):107–15. Epub 20111128. <https://doi.org/10.1016/j.ceb.2011.10.004> PMID: 22129583; PubMed Central PMCID: PMC3294052.
62. Ghosh S, Di Bartolo V, Tubul L, Shimoni E, Kartvelishvili E, Dadosh T, et al. ERM-Dependent Assembly of T Cell Receptor Signaling and Co-stimulatory Molecules on Microvilli prior to Activation. *Cell Rep.* 2020; 30(10):3434–47 e6. <https://doi.org/10.1016/j.celrep.2020.02.069> PMID: 32160548.
63. Yu Y, Zhu J, Mi LZ, Walz T, Sun H, Chen J, et al. Structural specializations of alpha(4)beta(7), an integrin that mediates rolling adhesion. *J Cell Biol.* 2012; 196(1):131–46. Epub 2012/01/11. <https://doi.org/10.1083/jcb.201110023> PMID: 22232704; PubMed Central PMCID: PMC3255974.
64. Wu H, Myszka DG, Tendian SW, Brouillette CG, Sweet RW, Chaiken IM, et al. Kinetic and structural analysis of mutant CD4 receptors that are defective in HIV gp120 binding. *Proc Natl Acad Sci U S A.* 1996; 93(26):15030–5. <https://doi.org/10.1073/pnas.93.26.15030> PMID: 8986758; PubMed Central PMCID: PMC26350.
65. Haynes BF, Gilbert PB, McElrath MJ, Zolla-Pazner S, Tomaras GD, Alam SM, et al. Immune-correlates analysis of an HIV-1 vaccine efficacy trial. *N Engl J Med.* 2012; 366(14):1275–86. <https://doi.org/10.1056/NEJMoa1113425> PMID: 22475592; PubMed Central PMCID: PMC3371689.
66. Zolla-Pazner S, deCamp AC, Cardozo T, Karasavvas N, Gottardo R, Williams C, et al. Analysis of V2 antibody responses induced in vaccinees in the ALVAC/AIDSVAX HIV-1 vaccine efficacy trial. *PLoS One.* 2013; 8(1):e53629. Epub 20130117. <https://doi.org/10.1371/journal.pone.0053629> PMID: 23349725; PubMed Central PMCID: PMC3547933.
67. Karasavvas N, Billings E, Rao M, Williams C, Zolla-Pazner S, Bailer RT, et al. The Thai Phase III HIV Type 1 Vaccine trial (RV144) regimen induces antibodies that target conserved regions within the V2 loop of gp120. *AIDS Res Hum Retroviruses.* 2012; 28(11):1444–57. Epub 20121004. <https://doi.org/10.1089/aid.2012.0103> PMID: 23035746; PubMed Central PMCID: PMC3484815.
68. Rolland M, Edlefsen PT, Larsen BB, Tovanabutra S, Sanders-Buell E, Hertz T, et al. Increased HIV-1 vaccine efficacy against viruses with genetic signatures in Env V2. *Nature.* 2012; 490(7420):417–20. Epub 20120910. <https://doi.org/10.1038/nature11519> PMID: 22960785; PubMed Central PMCID: PMC3551291.
69. Liao HX, Bonsignori M, Alam SM, McLellan JS, Tomaras GD, Moody MA, et al. Vaccine induction of antibodies against a structurally heterogeneous site of immune pressure within HIV-1 envelope protein variable regions 1 and 2. *Immunity.* 2013; 38(1):176–86. Epub 20130111. <https://doi.org/10.1016/j.immuni.2012.11.011> PMID: 23313589; PubMed Central PMCID: PMC3569735.
70. Wibmer CK, Richardson SI, Yolitz J, Cicala C, Arthos J, Moore PL, et al. Common helical V1V2 conformations of HIV-1 Envelope expose the alpha4beta7 binding site on intact virions. *Nat Commun.* 2018; 9(1):4489. Epub 20181026. <https://doi.org/10.1038/s41467-018-06794-x> PMID: 30367034; PubMed Central PMCID: PMC6203816.
71. Easterhoff D, Moody MA, Fera D, Cheng H, Ackerman M, Wiehe K, et al. Boosting of HIV envelope CD4 binding site antibodies with long variable heavy third complementarity determining region in the randomized double blind RV305 HIV-1 vaccine trial. *PLoS Pathog.* 2017; 13(2):e1006182. Epub 20170224. <https://doi.org/10.1371/journal.ppat.1006182> PMID: 28235027; PubMed Central PMCID: PMC5342261.
72. Tomaras GD, Plotkin SA. Complex immune correlates of protection in HIV-1 vaccine efficacy trials. *Immunol Rev.* 2017; 275(1):245–61. <https://doi.org/10.1111/immr.12514> PMID: 28133811; PubMed Central PMCID: PMC5330182.
73. Gray GE, Bekker LG, Laher F, Malahleha M, Allen M, Moodie Z, et al. Vaccine Efficacy of ALVAC-HIV and Bivalent Subtype C gp120-MF59 in Adults. *N Engl J Med.* 2021; 384(12):1089–100. <https://doi.org/10.1056/NEJMoa2031499> PMID: 33761206; PubMed Central PMCID: PMC7888373.
74. Agosto LM, Herring MB, Mothes W, Henderson AJ. HIV-1-Infected CD4+ T Cells Facilitate Latent Infection of Resting CD4+ T Cells through Cell-Cell Contact. *Cell Rep.* 2018; 24(8):2088–100. Epub 2018/08/23. <https://doi.org/10.1016/j.celrep.2018.07.079> PMID: 30134170.
75. Pancera M, Zhou T, Druz A, Georgiev IS, Soto C, Gorman J, et al. Structure and immune recognition of trimeric pre-fusion HIV-1 Env. *Nature.* 2014; 514(7523):455–61. Epub 20141008. <https://doi.org/10.1038/nature13808> PMID: 25296255; PubMed Central PMCID: PMC4348022.
76. Kwon YD, Pancera M, Acharya P, Georgiev IS, Crooks ET, Gorman J, et al. Crystal structure, conformational fixation and entry-related interactions of mature ligand-free HIV-1 Env. *Nat Struct Mol Biol.* 2015; 22(7):522–31. Epub 20150622. <https://doi.org/10.1038/nsmb.3051> PMID: 26098315; PubMed Central PMCID: PMC4706170.
77. Julien JP, Cupo A, Sok D, Stanfield RL, Lyumkis D, Deller MC, et al. Crystal structure of a soluble cleaved HIV-1 envelope trimer. *Science.* 2013; 342(6165):1477–83. Epub 20131031. <https://doi.org/10.1126/science.1245625> PMID: 24179159; PubMed Central PMCID: PMC3886632.

78. Gao N, Gai Y, Meng L, Wang C, Wang W, Li X, et al. Development of Neutralization Breadth against Diverse HIV-1 by Increasing Ab-Ag Interface on V2. *Adv Sci (Weinh)*. 2022; 9(15):e2200063. Epub 20220323. <https://doi.org/10.1002/advs.202200063> PMID: 35319830; PubMed Central PMCID: PMC9130890.
79. Myszka DG, Jonsen MD, Graves BJ. Equilibrium analysis of high affinity interactions using BIACORE. *Anal Biochem*. 1998; 265(2):326–30. <https://doi.org/10.1006/abio.1998.2937> PMID: 9882410.